

## Supplementary Information

for

### Temperature - pH and H-bond Synergism for Peptide Bond Formation: Synthesis of Sequence Specific Tetra- and Penta-peptides Without Using Coupling Reagent

Palwinder Singh<sup>\*†</sup>, Amrinder Singh<sup>a†</sup>, Sukhmeet Kaur<sup>a†</sup>, Venus Singh Mithu<sup>a†</sup>, Manpreet S Bhatti<sup>b‡</sup>

<sup>†</sup>Department of Chemistry, UGC Sponsored Centre for Advanced Studies, Guru Nanak Dev University, Amritsar, Punjab, India

<sup>‡</sup>Department of Botanical and Environmental Sciences, Guru Nanak Dev University, Amritsar, India

#### Table of contents

content	Page no.
<b>Method details</b>	<b>2</b>
<b>Scheme S1.</b> Stepwise elongation of the peptide	<b>3</b>
<b>Chart S1.</b> Reaction mixture under basic conditions	<b>4</b>
<b>Figure S1.</b> High resolution mass spectrum of the reaction mixtures	<b>4</b>
<b>Figure S2.</b> LC chromatogram of diketopiperazine <b>2</b>	<b>5</b>
<b>Figure S3.</b> Mass spectrum of freshly prepared (without heating) solution of L-pro and L-hisHCl	<b>5</b>
<b>Figure S4.</b> <sup>1</sup> H NMR Spectrum of N-Cbz-VG-OMe (CDCl <sub>3</sub> as solvent)	<b>6</b>
<b>Figure S5.</b> <sup>13</sup> C NMR Spectrum of N-Cbz-VG-OMe (CDCl <sub>3</sub> as solvent)	<b>6</b>
<b>Figure S6.</b> DEPT-135 NMR Spectrum of N-Cbz-VG-OMe (CDCl <sub>3</sub> as solvent)	<b>7</b>
<b>Figure S7.</b> DEPT-90 NMR Spectrum of N-Cbz-VG-OMe (CDCl <sub>3</sub> as solvent)	<b>7</b>
<b>Figure S8.</b> A) Pareto chart showing the significant process variables. B) Two factor interaction plot showing effect of reaction temperature and pH vs. yield.	<b>8</b>
<b>Figure S9.</b> LC, NMR of peptides	<b>9</b>
<b>Figure S10-13.</b> NMR spectrum of N-Cbz-VGL-OMe (CDCl <sub>3</sub> as solvent)	<b>10-11</b>
<b>Figure S14-17.</b> NMR spectrum of N-Cbz-VGLA-OMe (CDCl <sub>3</sub> as solvent)	<b>12-13</b>
<b>Figure 18.</b> NMR spectrum of N-Cbz-GPVAI(OMe) pentapeptide.	<b>14-17</b>
<b>Figure S19.</b> LC-MS of Cbz-L-pro-DL-val dipeptide.	<b>17</b>
<b>Figure 20.</b> Mechanism of peptide bond formation.	<b>18</b>
<b>Figure S21.</b> Mass spectrum of solution of N-Cbz-gly and ala at pH 7.5-10.0	<b>19</b>
<b>Figure S22.</b> Half Normal % Probability graph showing significant process variables	<b>19</b>
<b>Table S1.</b> Experimental data for reaction temperature, pH, reaction time and reactant concentration for un-catalyzed aqueous phase formation of N-Cbz-val-gly(OMe).	<b>20-21</b>
<b>Table S2.</b> Fractional factorial design (Resolution-IV) showing four independent variables along with actual and predicted yield	<b>22</b>
<b>Table S3.</b> Comparison of optical rotation of dipeptides obtained through two different experiments.	<b>22</b>
<b>Table S4.</b> ANOVA table and model statistics for yield	<b>23</b>
<b>General experimental procedure</b>	<b>23-27</b>

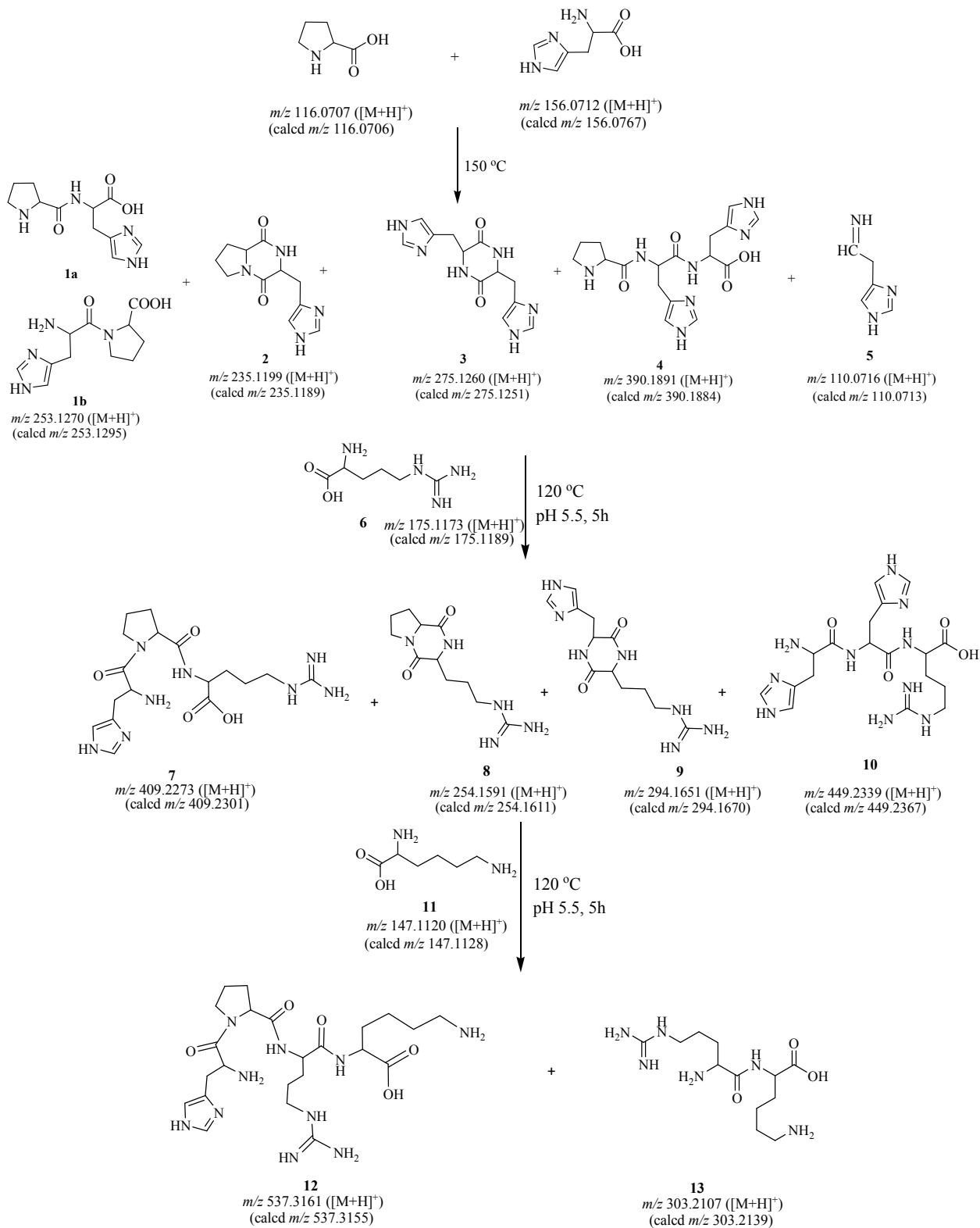
## Method details

### Mass spectrometry.

Mass spectra were recorded on Bruker MicroTOF QII mass spectrometer (Bruker Daltonik, Bremen, Germany). Machine was calibrated with sodium formate. Using KdScientific automated pump with flow rate 180  $\mu\text{L}/\text{h}$ , 50  $\mu\text{M}$  solution in acetonitrile-water-formic acid (7:2.9:0.1) was injected to electrospray ionization source. Desolvation was performed with dry  $\text{N}_2$  gas heated at 180  $^\circ\text{C}$ . Various parameters of the mass spectrometer were optimized for maximum ion abundance of peptide species. Typically, the capillary voltage was 4500 V and vacuum was maintained at  $3\text{-}4 \times 10^{-7}$  mbar. By varying the collision RF and other ion transfer parameters, mass spectra were recorded in different mass ranges so that mass peaks in lower mass range as well as higher mass range are picked up. Fragmentation was performed in the collision cell using Ar as the energized gas and collision energy was varied for optimum fragmentation of the molecular ion.

**LC-MS.** Peptide solutions were also prepared in the same solvent system as for amino acids with 50  $\mu\text{M}$  concentration and mass spectra were recorded with the instrument parameters as mentioned above. For LC-MS, Dionex Ultimate 3000 system was linked to mass spectrometer. Chirobiotic<sup>®</sup> T 10  $\mu\text{m}$  chiral HPLC column (25 cm x 4.6 mm) was used which also ensured the the chiral purity of the peptides. Acetonitrile-water (1:1) was used as eluent. 2  $\mu\text{L}$  of sample (injection volume) was loaded to the column, flow rate was kept 0.2 ml and absorbance was set at 200, 220 and 254 nm. Sodium formate was used as internal calibrant.

**NMR, IR, optical rotation.** NMR spectra were recorded on Bruker 500 MHz NMR spectrometer. Depending on solubility of the peptide, NMR spectra were recorded in  $\text{CDCl}_3$  and/or  $\text{DMSO-d}_6$  with TMS as internal standard. Optical rotation was recorded on AT-100 Atago automatic polarimeter. Flash chromatography was performed using Biotage Isolera One 2.0.8 model in isocratic mode with ethyl acetate – hexane as eluent.



**Scheme S1.** Stepwise elongation of the peptide.

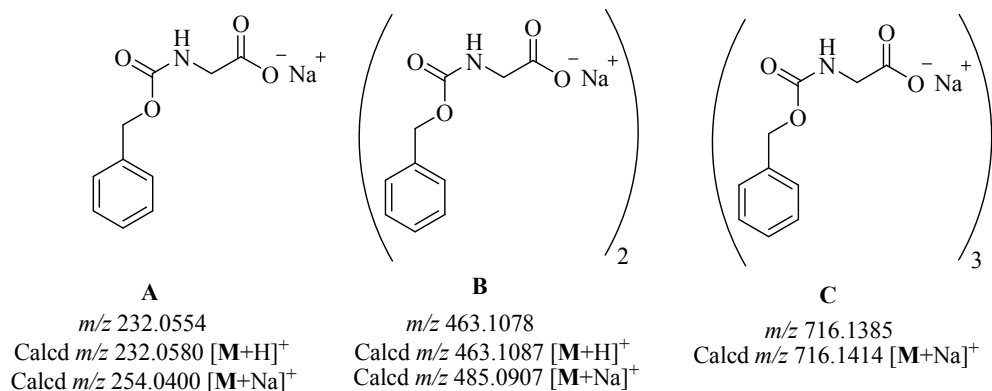


**Chart S1.** Formation of various species of N-Cbz-gly under basic conditions as detected from mass spectrum of solution of N-Cbz-gly and ala at pH 8.0-10.0 (Figure S19).

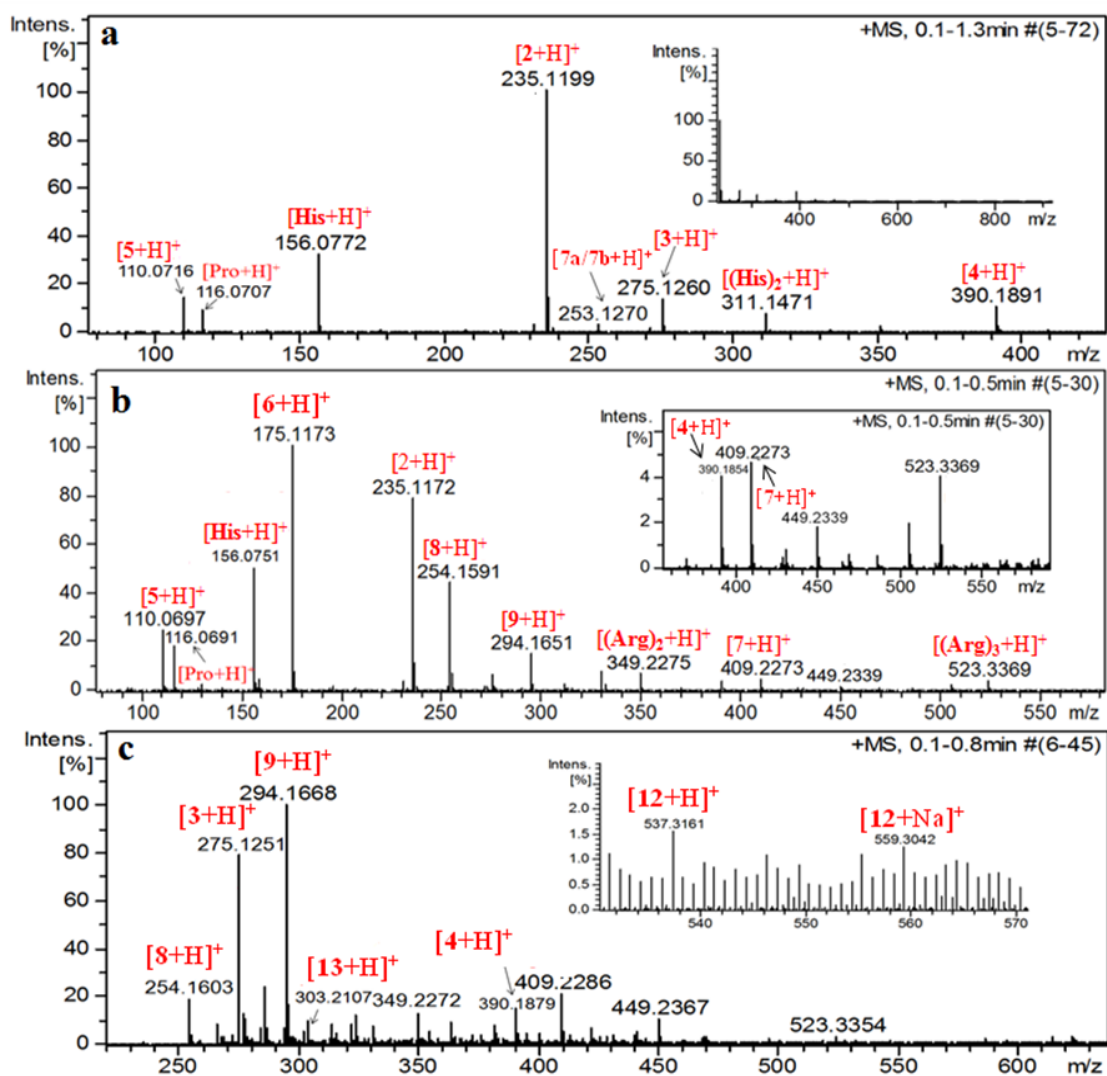


**Figure S1.** High resolution mass spectrum of the reaction mixtures heated at 120 °C for 3h: a) L-pro and L-his.HCl, b) addition of L-arg.HCl to the reaction mixture (a), c) addition of L-lys.HCl to the reaction mixture of (b).

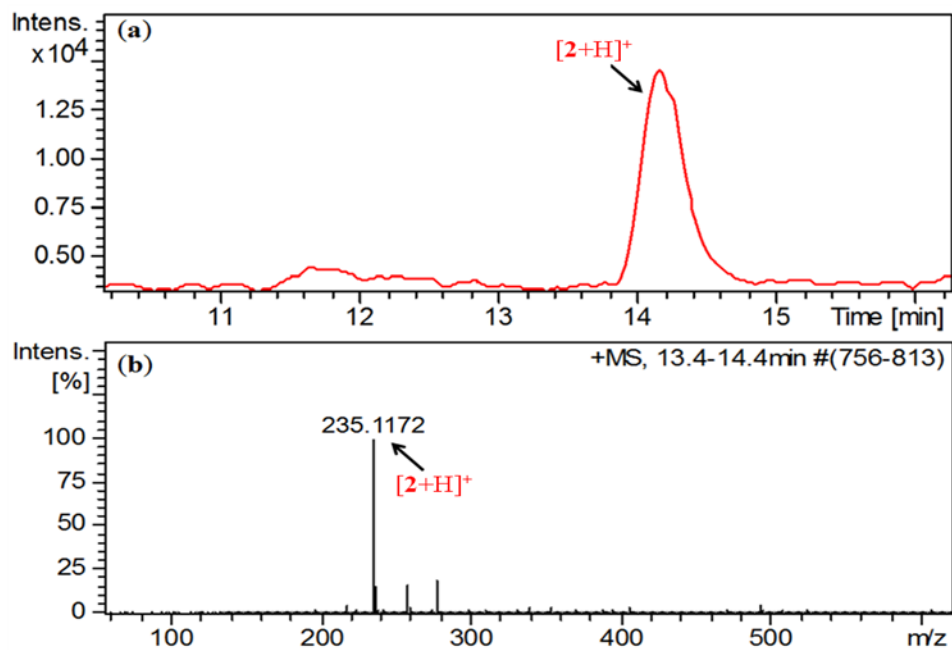


**Figure S2.** (a) LC chromatogram of diketopiperazine **2**, (b) corresponding mass spectrum.

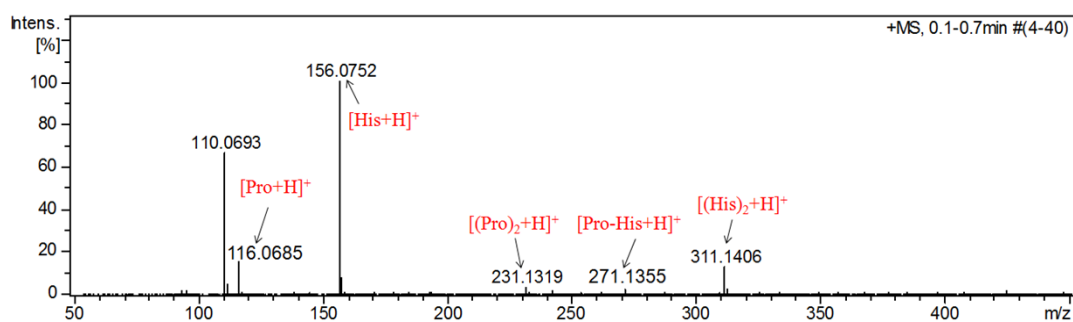


**Figure S3.** Mass spectrum of freshly prepared (without heating) solution of L-pro and L-hisHCl. Peak at  $m/z$  271.1355 corresponds to mass of pro – his adduct (calcd  $m/z$  271.1400  $[M+H]^+$ ).

AMR-VG-OMe

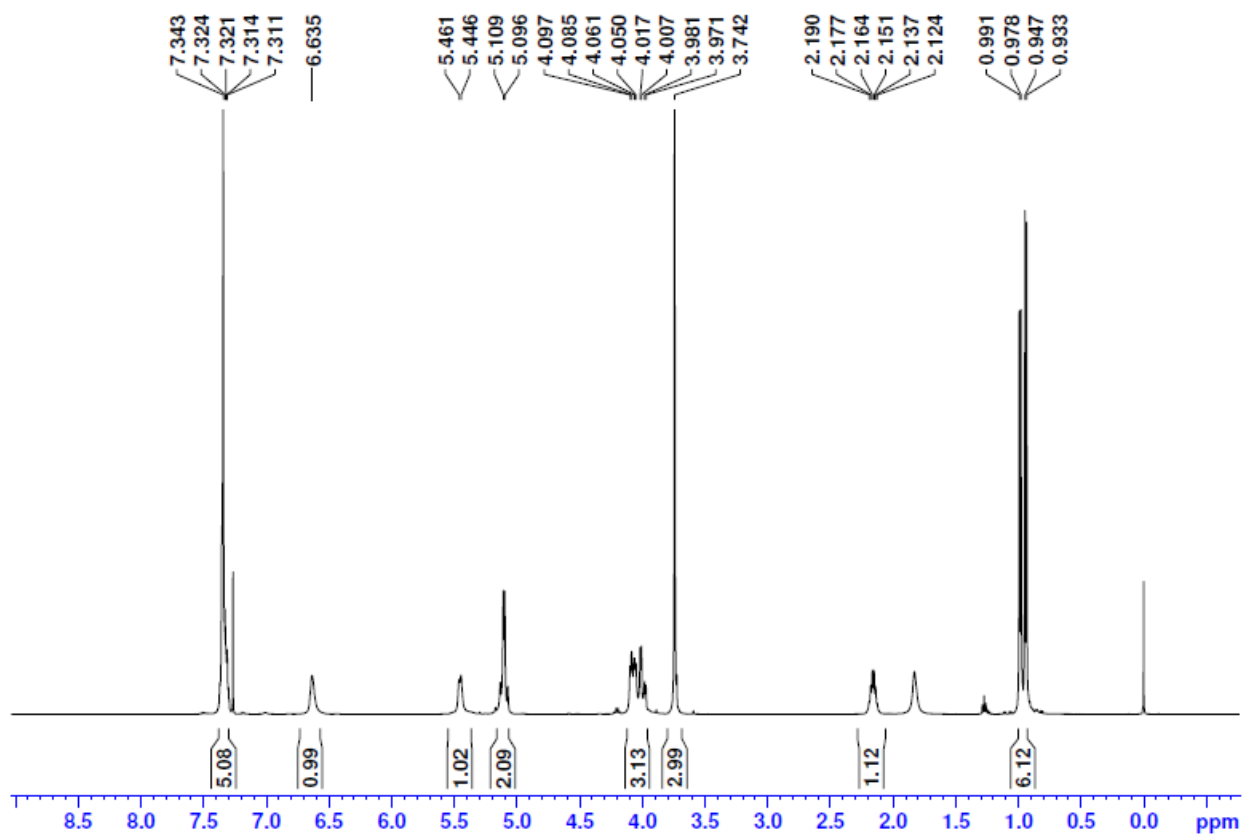


Figure S4. <sup>1</sup>H NMR Spectrum of N-Cbz-VG-OMe (CDCl<sub>3</sub> as solvent).

AMR\_VG\_OMe

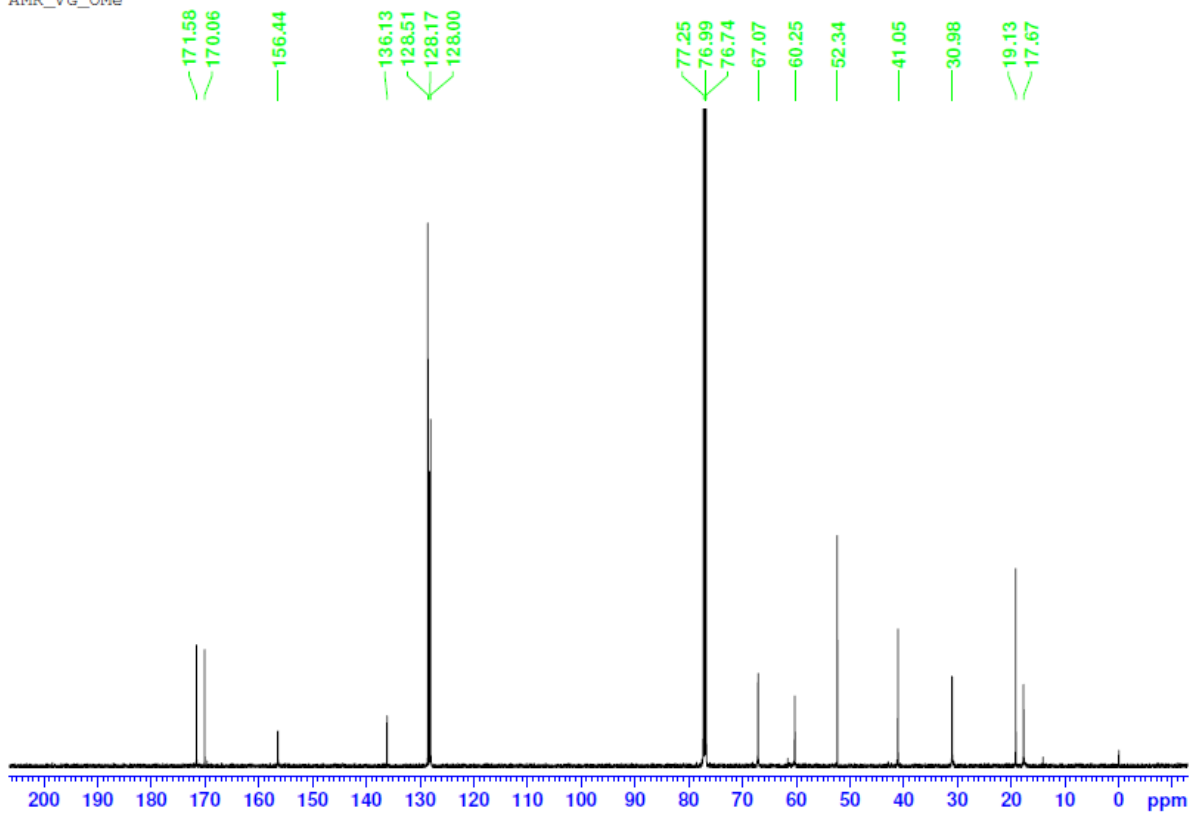
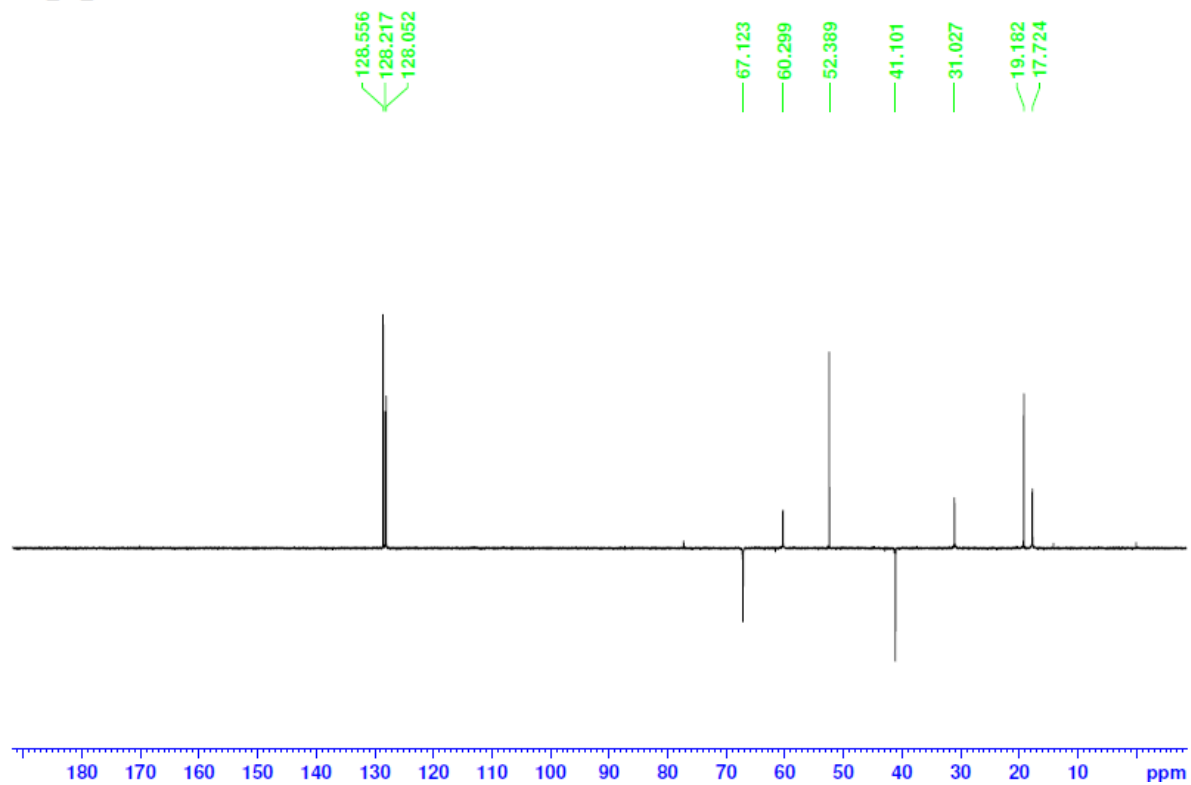


Figure S5. <sup>13</sup>C NMR Spectrum of N-Cbz-VG-OMe (CDCl<sub>3</sub> as solvent).

AMR\_VG\_OMe



**Figure S6.** DEPT-135 NMR Spectrum of N-Cbz-VG-OMe (CDCl<sub>3</sub> as solvent).

AMR\_VG\_OMe

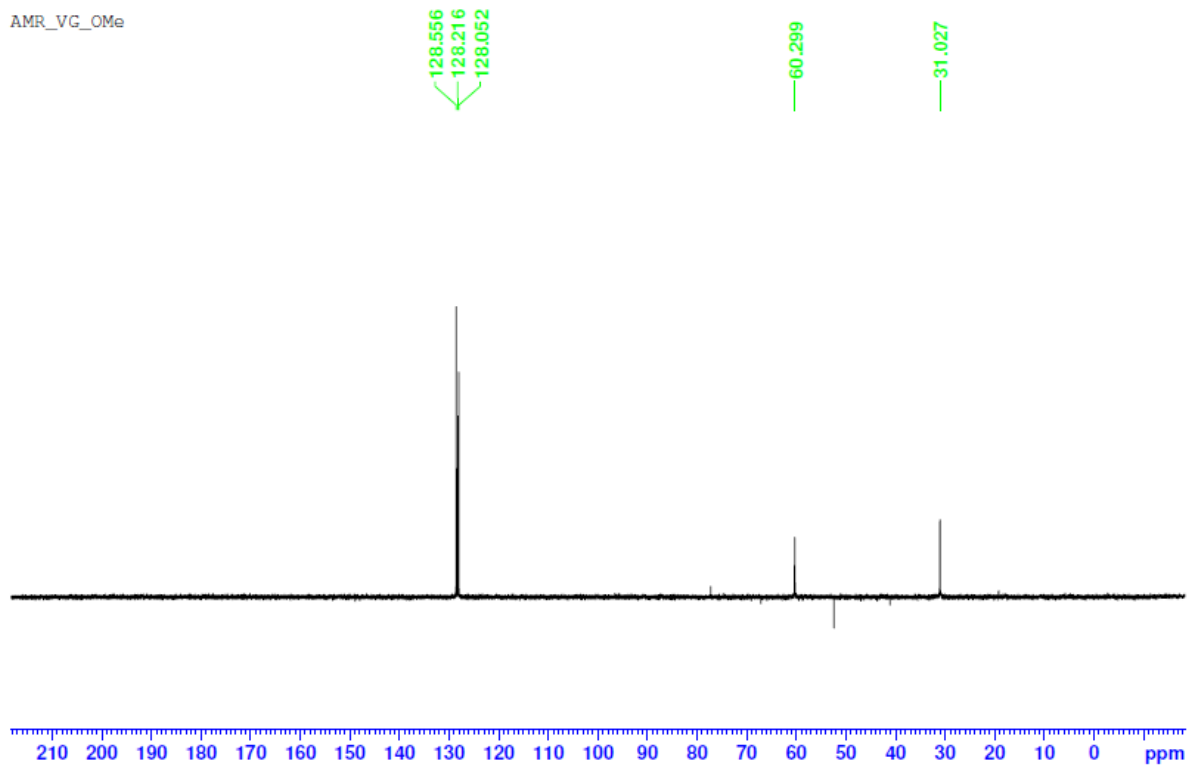


**Figure S7.** DEPT-90 NMR Spectrum of N-Cbz-VG-OMe (CDCl<sub>3</sub> as solvent).

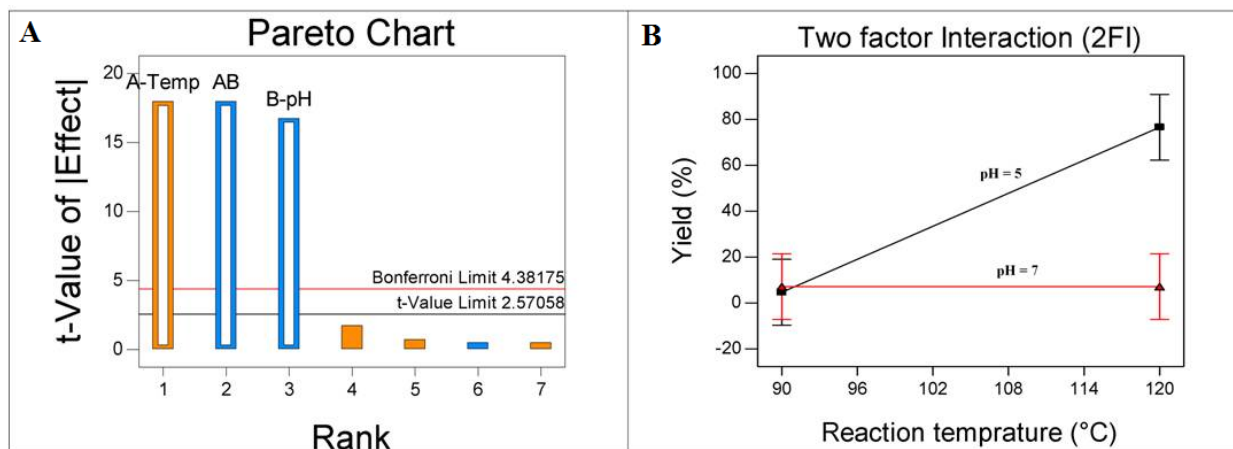


**Figure S8.** A) Pareto chart showing the significant process variables. B) Two factor interaction plot showing effect of reaction temperature and pH vs. yield.



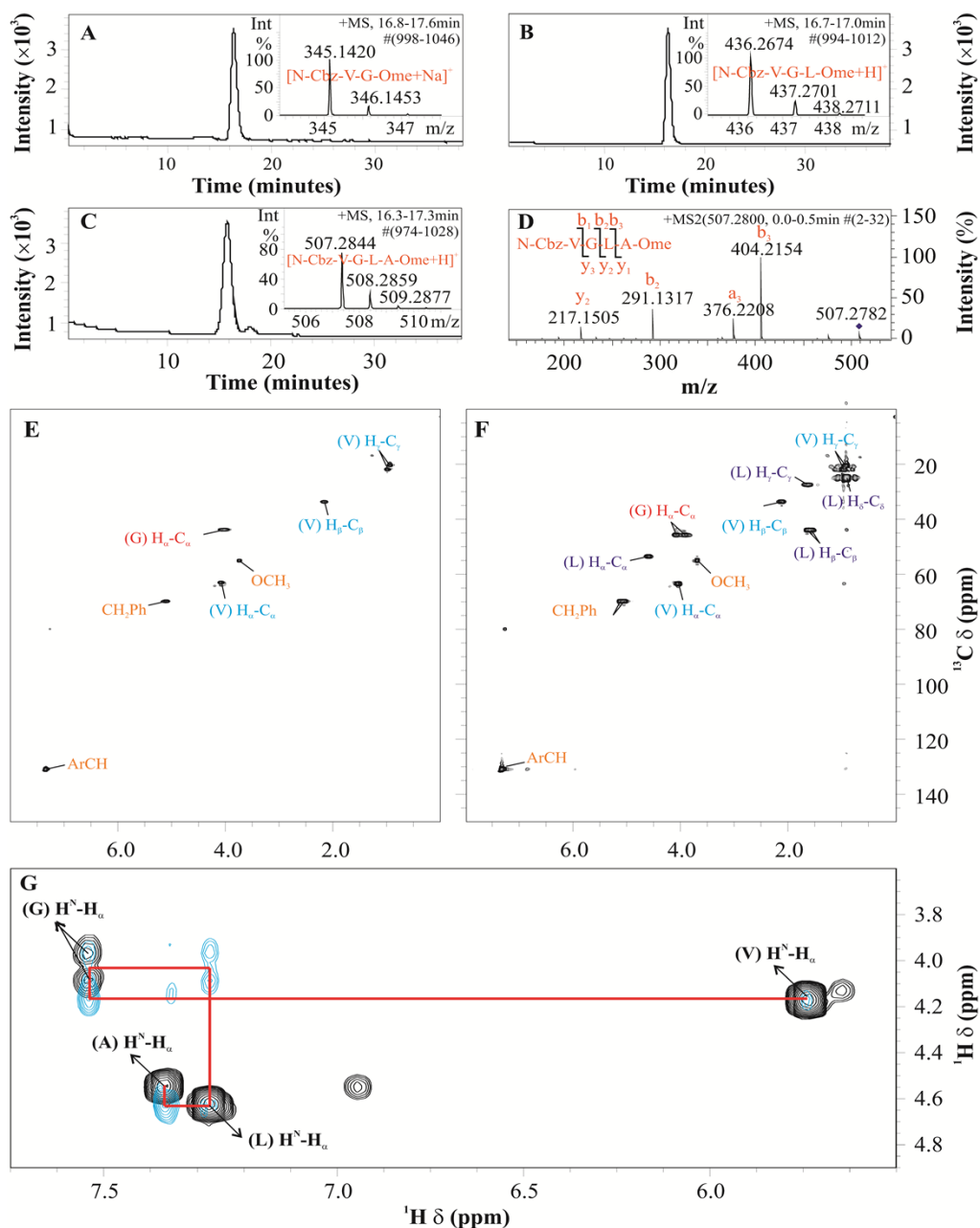


**Figure S9.** A) LC-MS of N-Cbz-VG-OME dipeptide; B) LC-MS of N-Cbz-VGL-OME tripeptide; C) LC-MS of N-Cbz-VGLA-OME tetrapeptide; D) Fragmentation pattern of N-Cbz-VGLA-OME tetrapeptide; E)  $^1\text{H}$ - $^{13}\text{C}$  HSQC NMR spectrum of N-Cbz-VG-OME dipeptide; F)  $^1\text{H}$ - $^{13}\text{C}$  HSQC NMR spectrum of N-Cbz-VGL-OME tripeptide; G) Overlap of  $^1\text{H}$ - $^1\text{H}$  COSY (Black) and  $^1\text{H}$ - $^1\text{H}$  ROESY (Blue) NMR spectra showing the sequence of N-Cbz-VGLA-OME tetrapeptide.

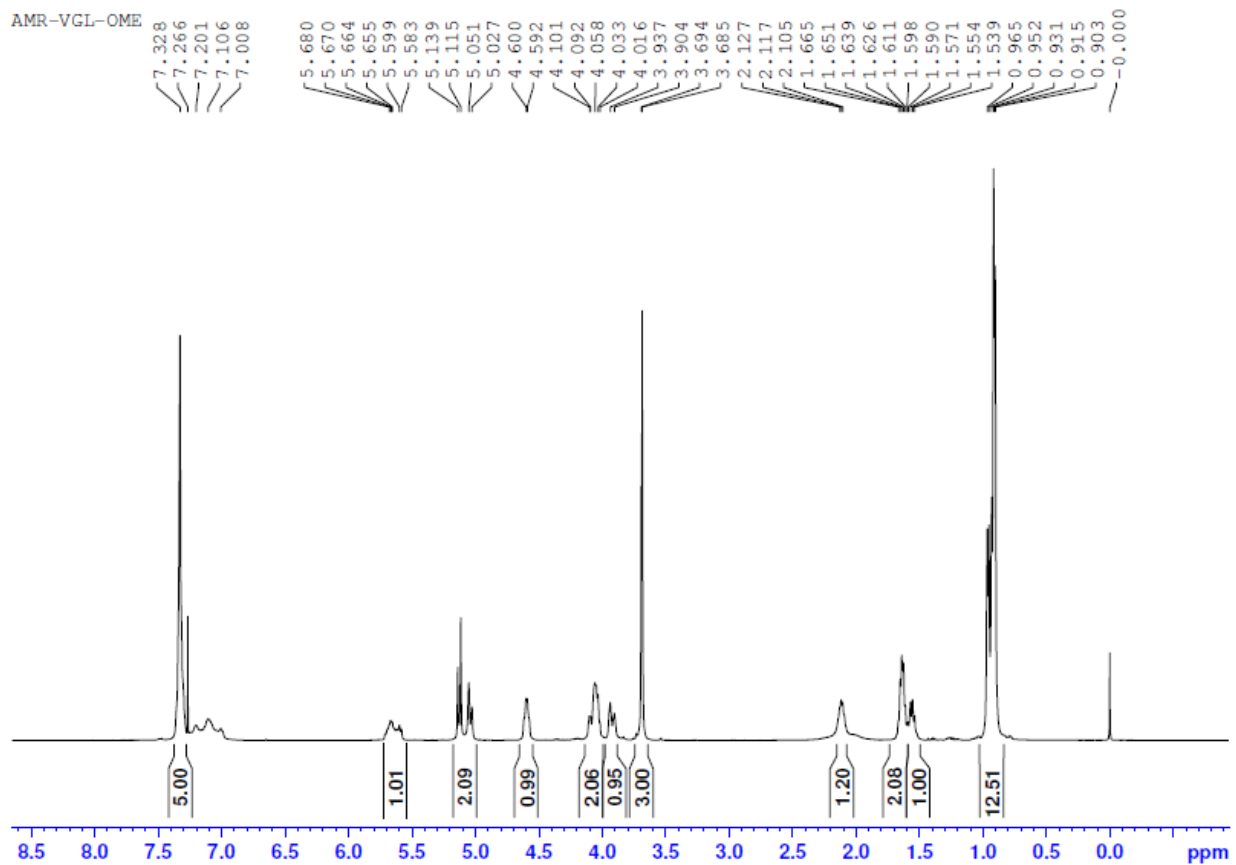


**Figure S10.**  $^1\text{H}$  NMR spectrum of N-Cbz-VGL-OMe ( $\text{CDCl}_3$  as solvent).

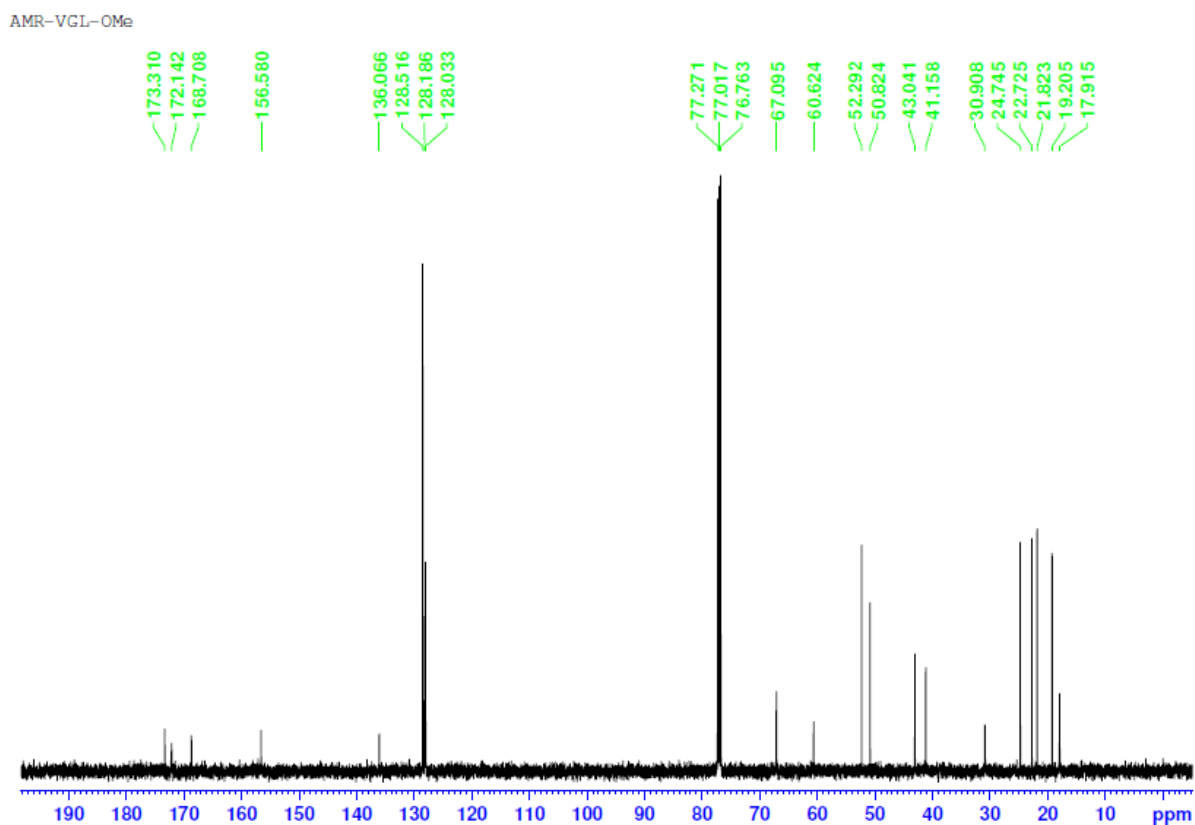


**Figure S11.**  $^{13}\text{C}$  NMR spectrum of N-Cbz-VGL-OMe ( $\text{CDCl}_3$  as solvent).

AMR-VGL-OMe

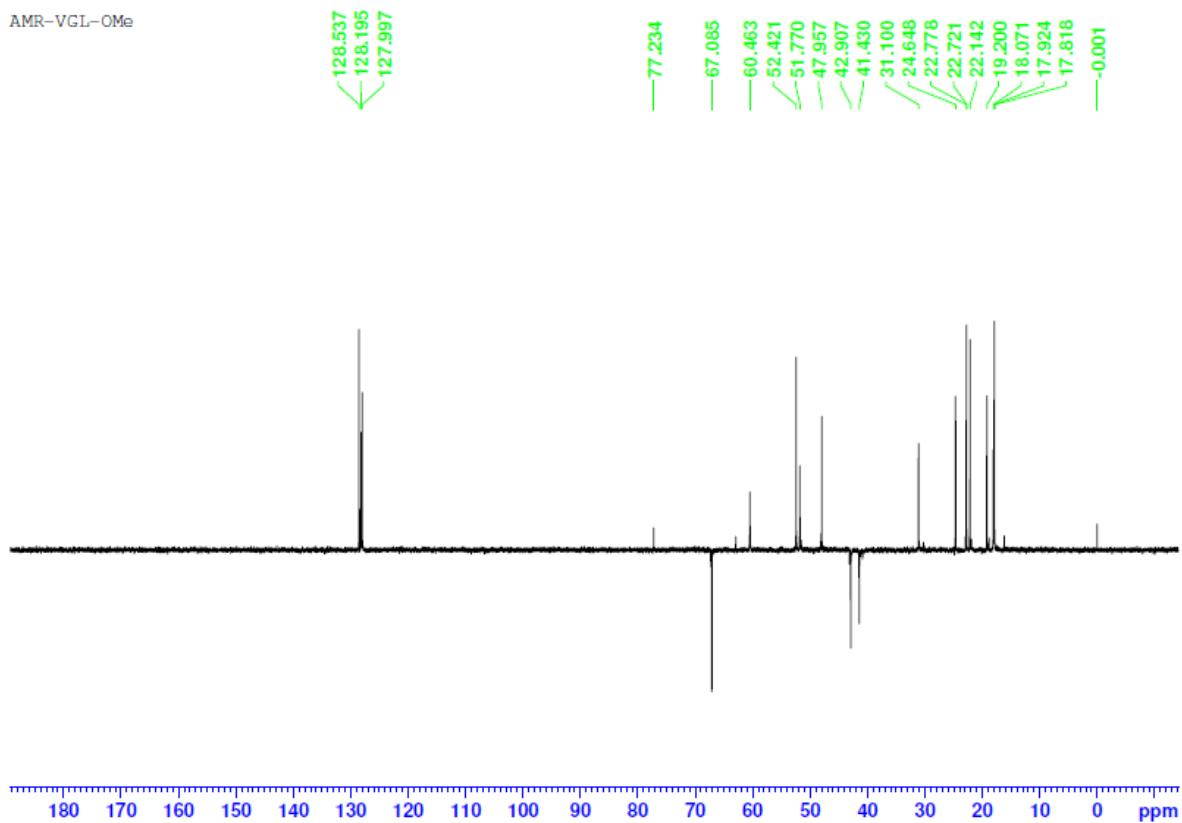


**Figure S12.** DEPT-135 NMR Spectrum of N-Cbz-VGL-OMe (CDCl<sub>3</sub> as solvent).

VGL-OMe

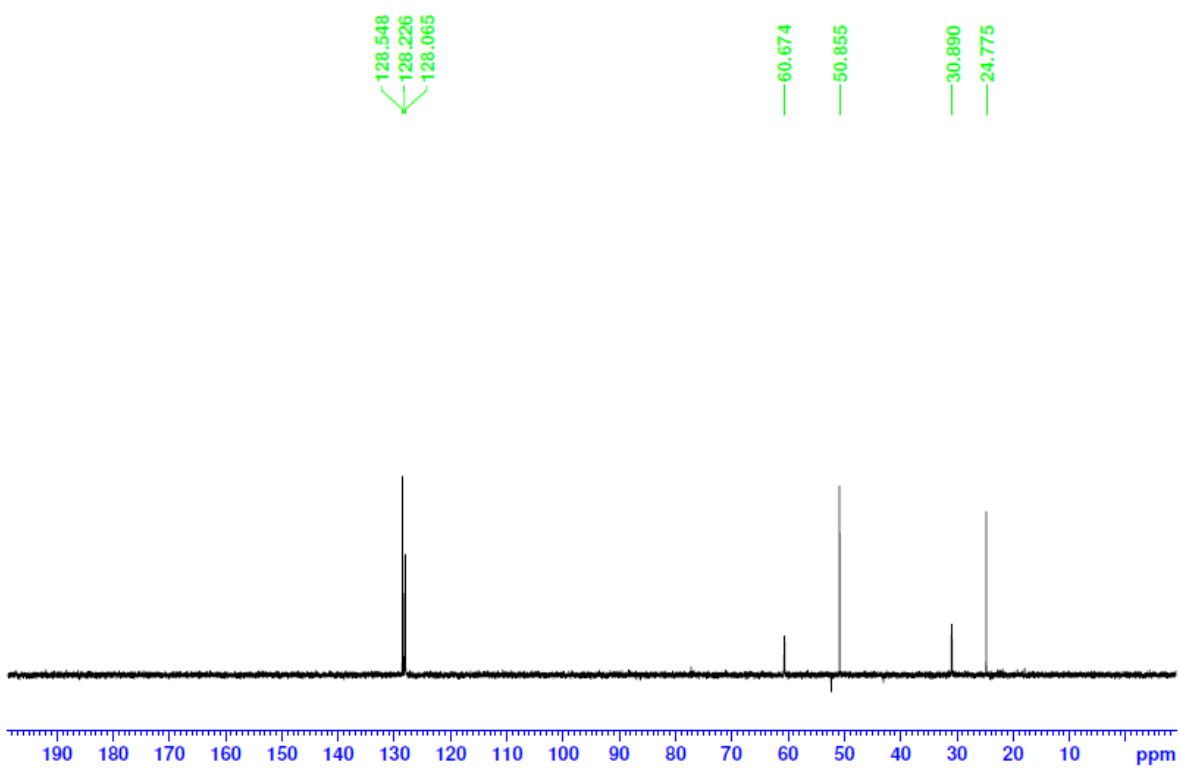


**Figure S13.** DEPT-90 NMR Spectrum of N-Cbz-VGL-OMe (CDCl<sub>3</sub> as solvent).

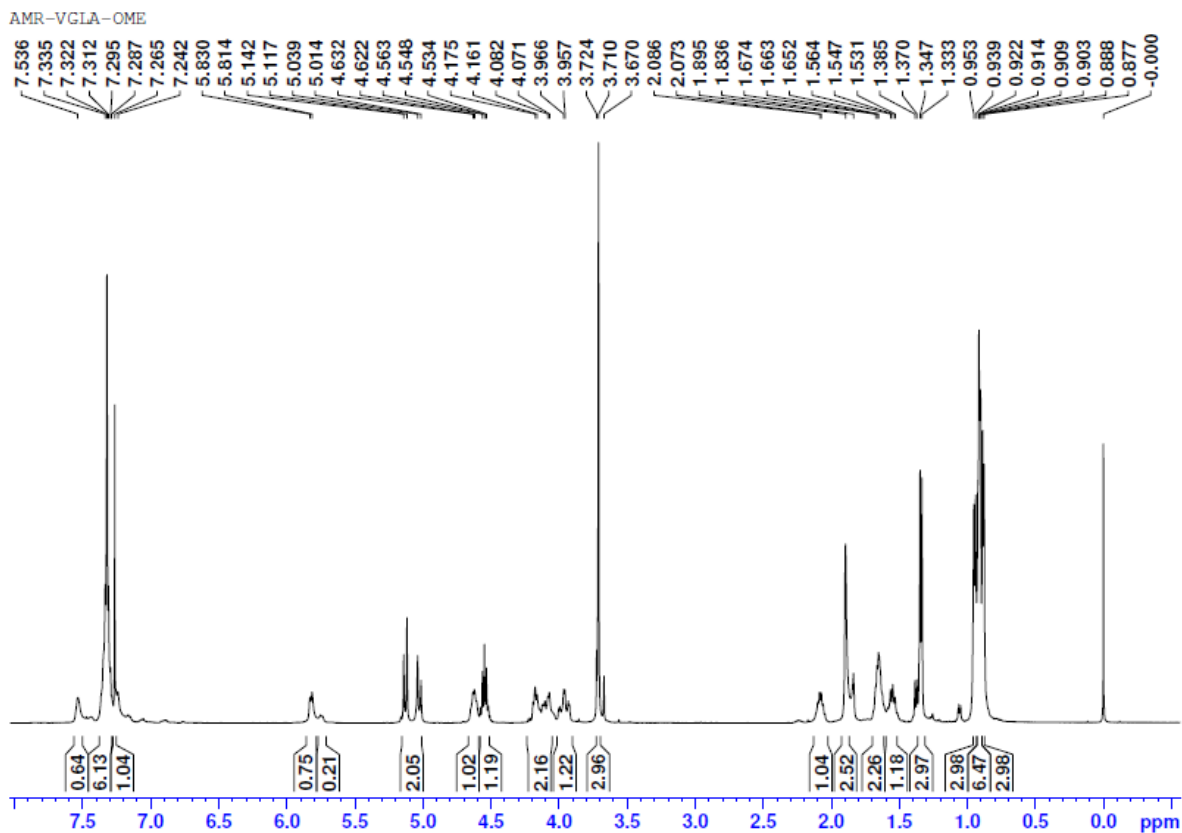


Figure S14.  $^1\text{H}$  NMR spectrum of N-Cbz-VGLA-OMe ( $\text{CDCl}_3$  as solvent).

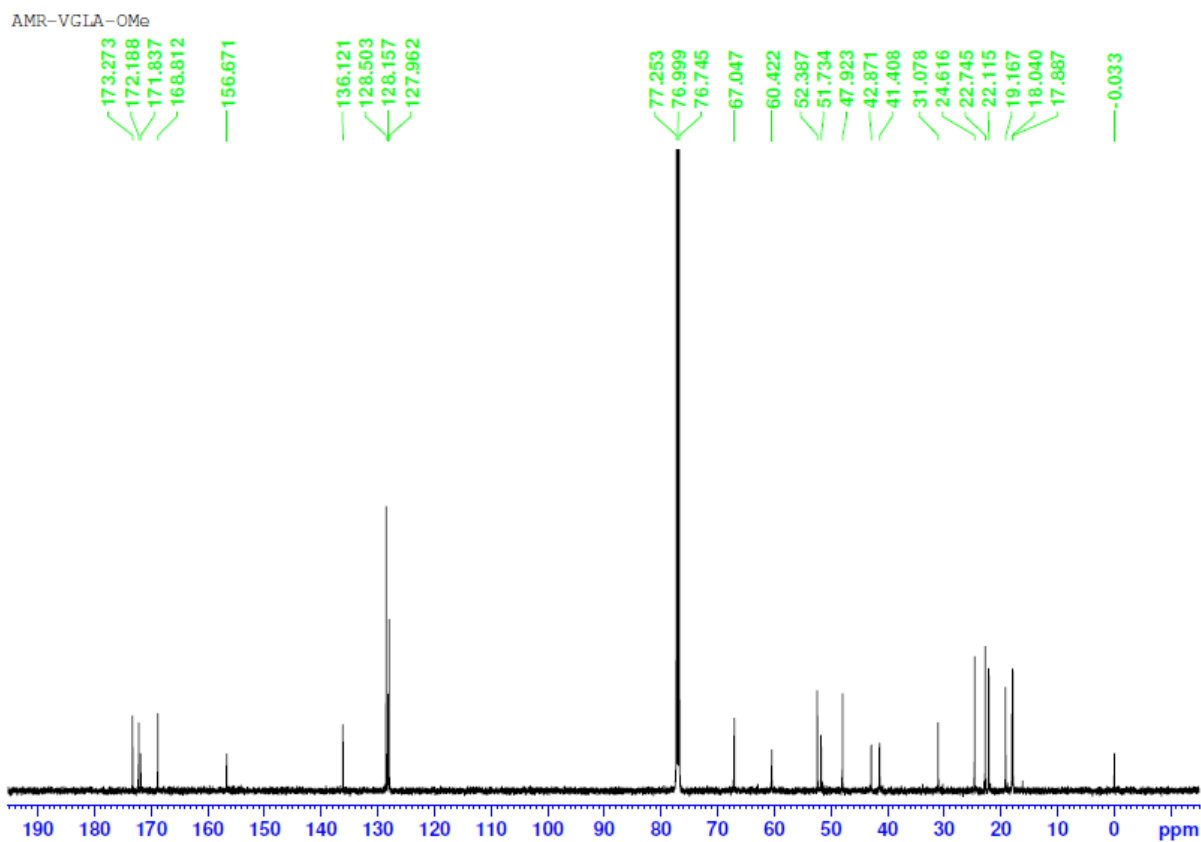


Figure S15.  $^{13}\text{C}$  NMR spectrum of N-Cbz-VGLA-OMe ( $\text{CDCl}_3$  as solvent).

AMR-VGLA-OMe

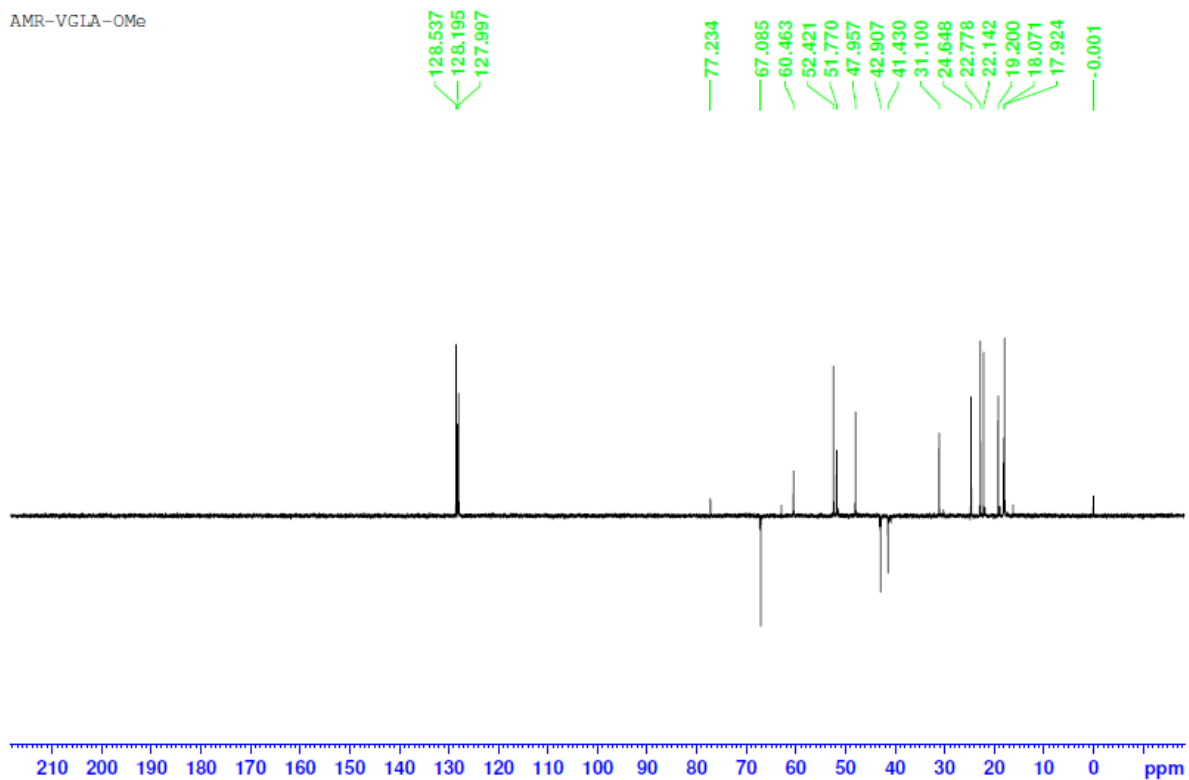


Figure S16. DEPT-135 NMR spectrum of N-Cbz-VGLA-OMe ( $\text{CDCl}_3$  as solvent).

VGLA-OMe

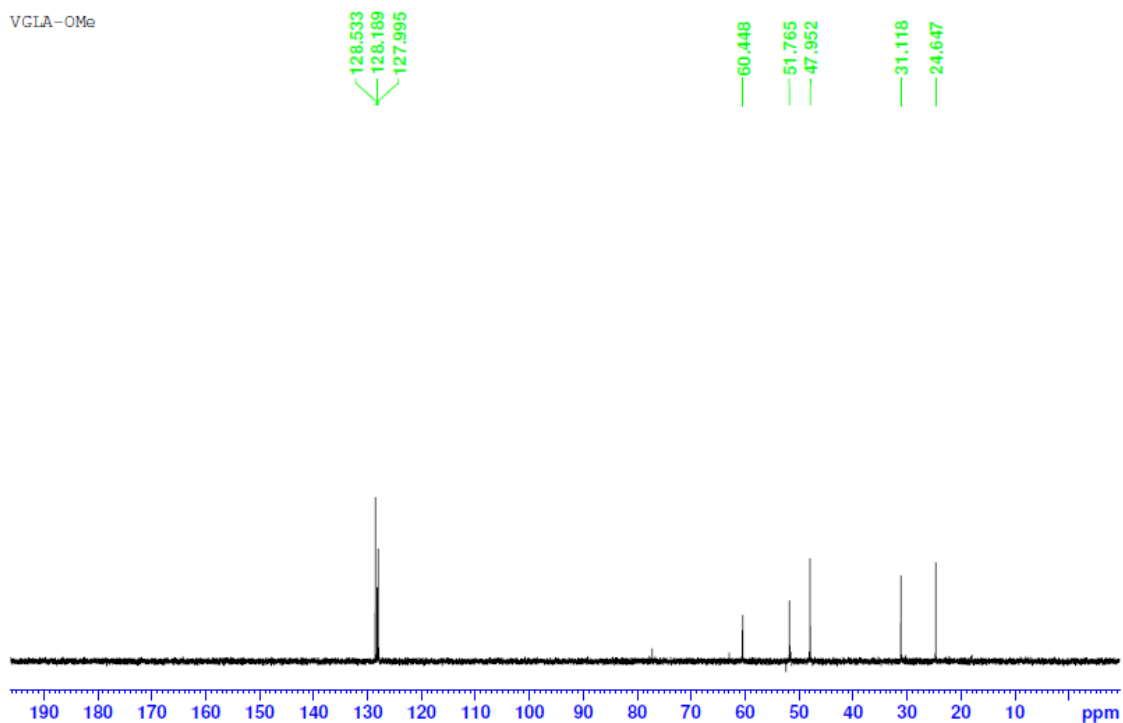


Figure S17. DEPT-90 NMR spectrum of N-Cbz-VGLA-OMe ( $\text{CDCl}_3$  as solvent).

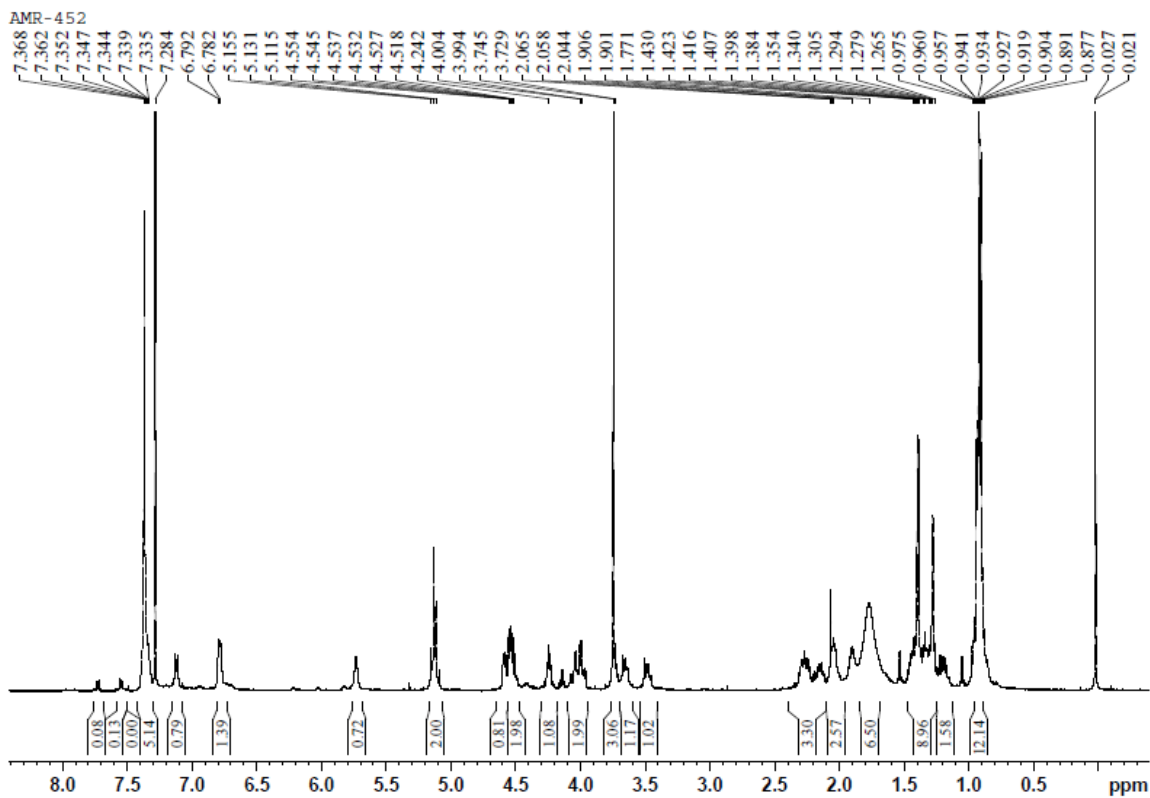


Figure S18a.  $^1\text{H}$  NMR spectrum of N-Cbz-GPVAI(OMe) pentapeptide.

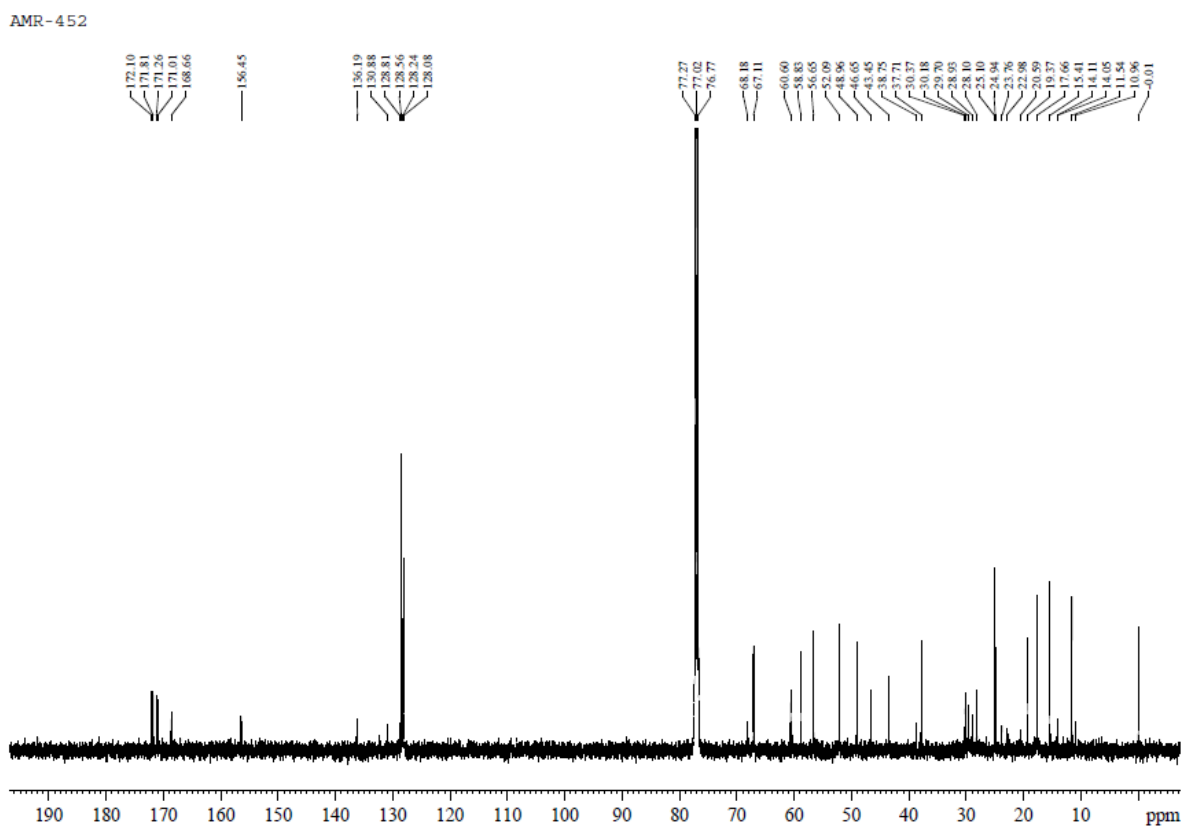
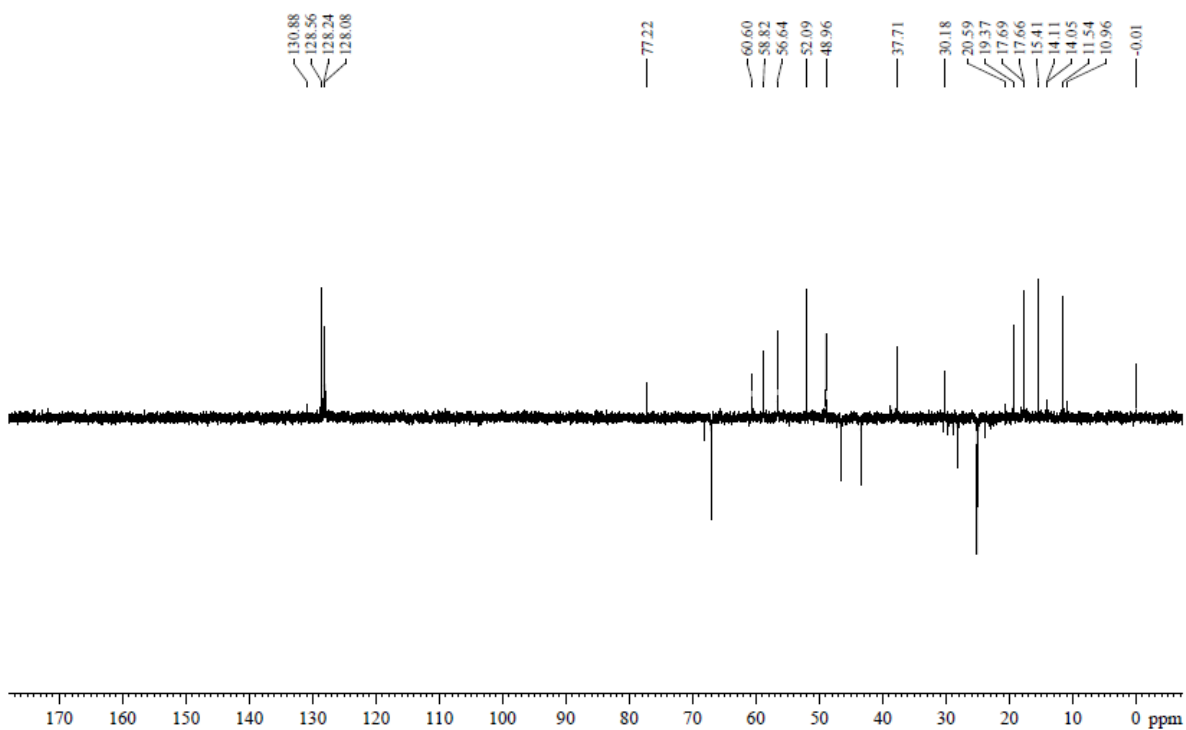
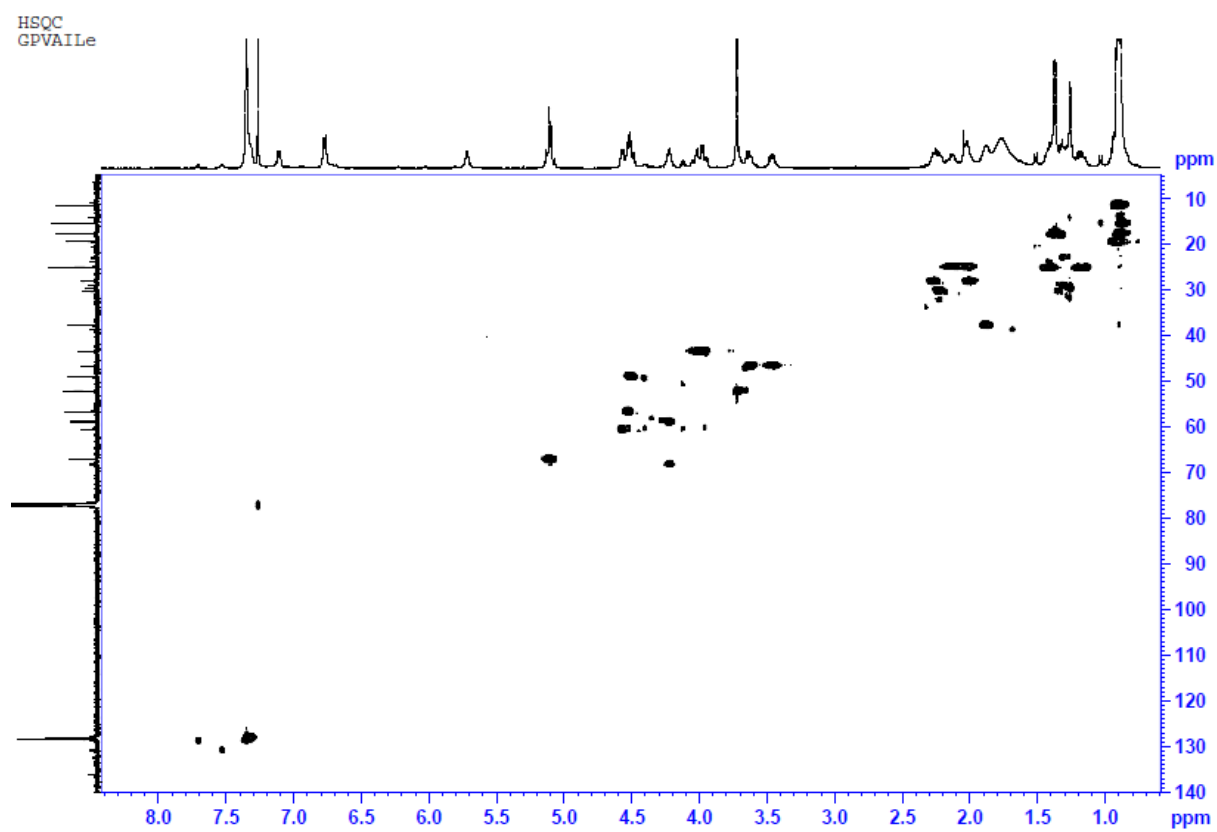


Figure S18b.  $^{13}\text{C}$  NMR spectrum of N-Cbz-GPVAI(OMe) pentapeptide



**Figure S18c.**  $^{13}\text{C}$ -DEPT135 spectrum of N-Cbz-GPVAI(OMe) pentapeptide.



**Figure S18d.** HSQC NMR spectrum of N-Cbz-GPVAI(OMe) pentapeptide.

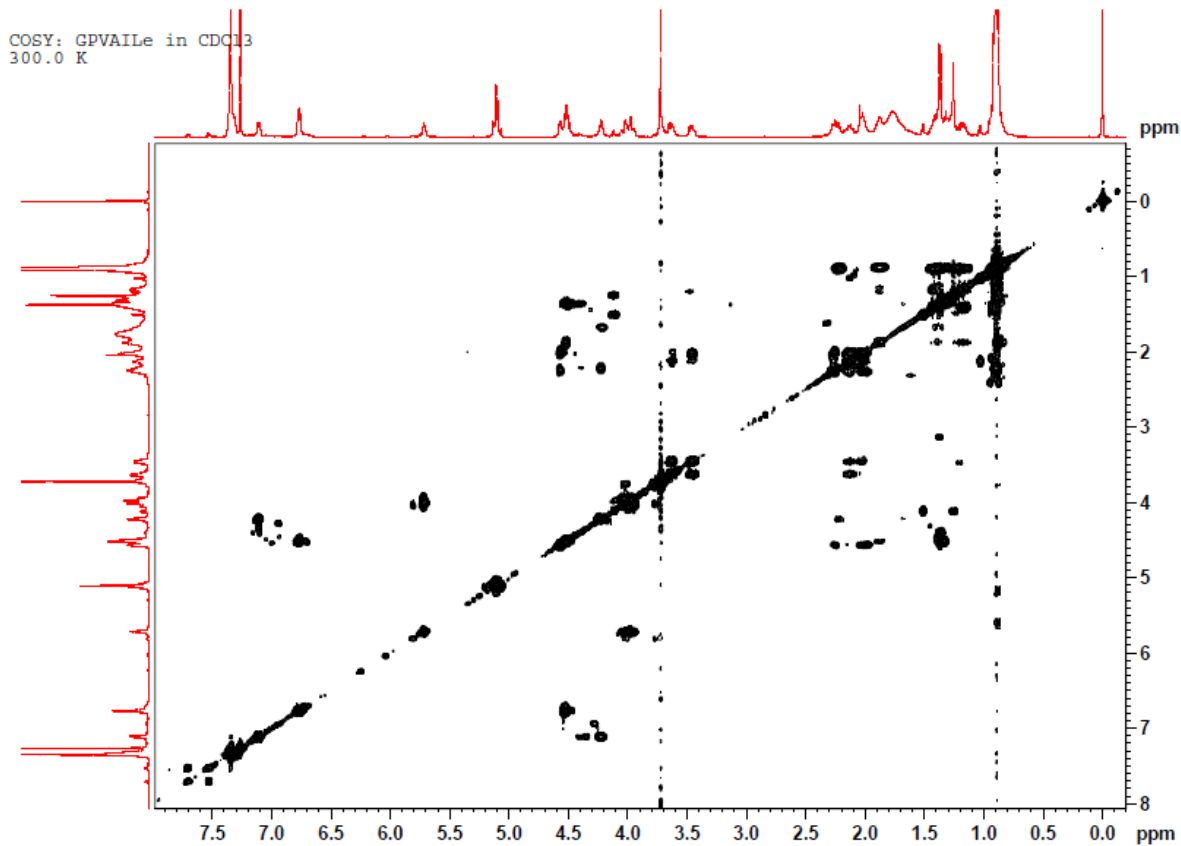


**Figure S18e.** <sup>1</sup>H-<sup>1</sup>H COSY spectrum of N-Cbz-GPVAI(OMe) pentapeptide.

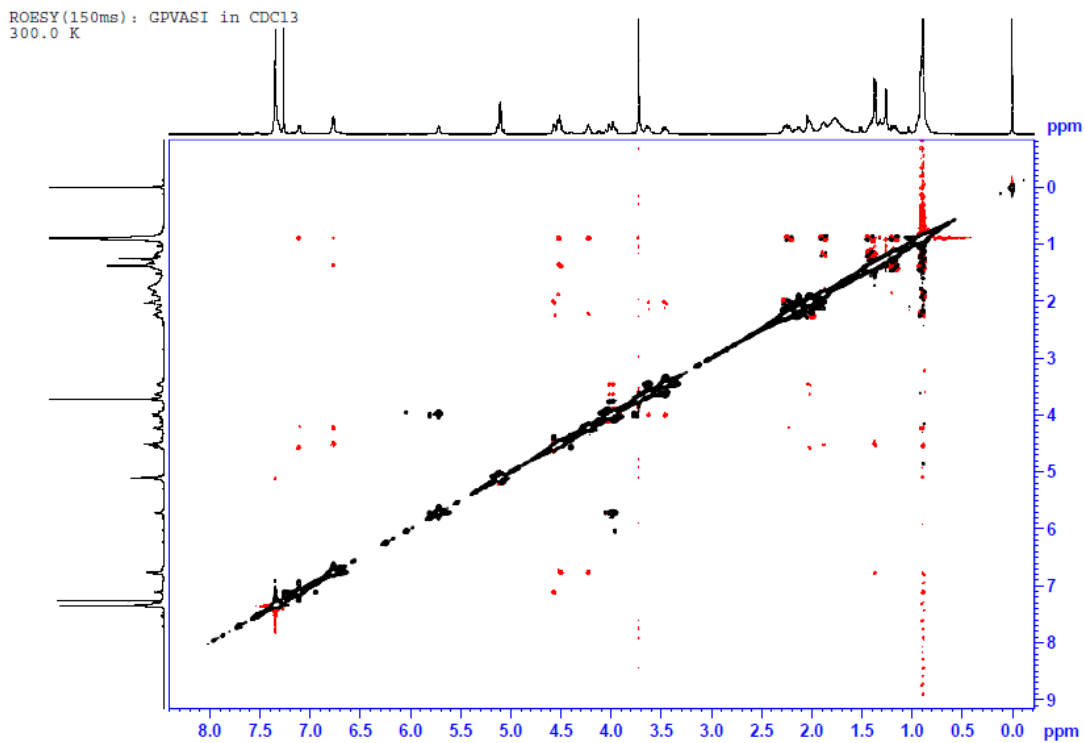


**Figure S18f.** ROESY spectrum of N-Cbz-GPVAI(OMe) pentapeptide.



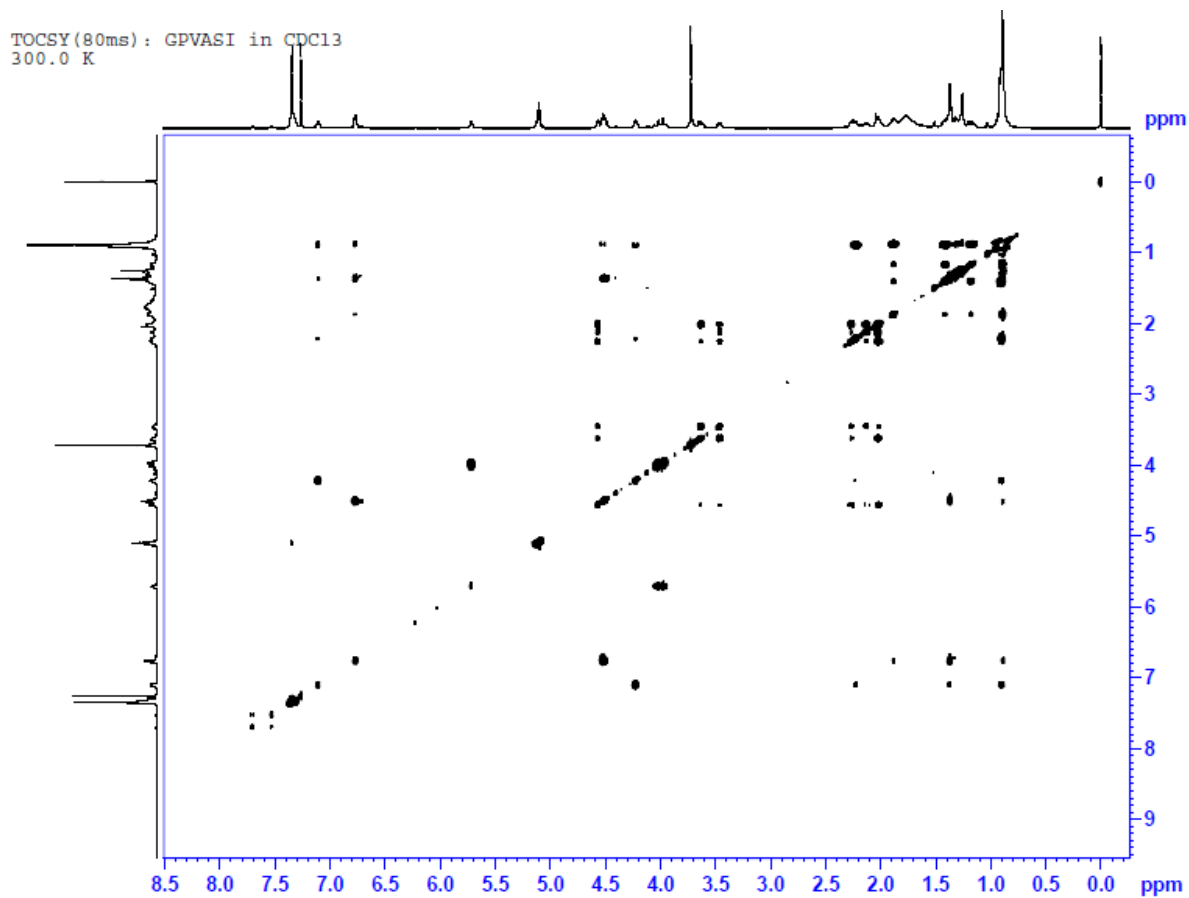


**Figure S18g.** TOCSY spectrum of N-Cbz-GPVAI(OMe) pentapeptide

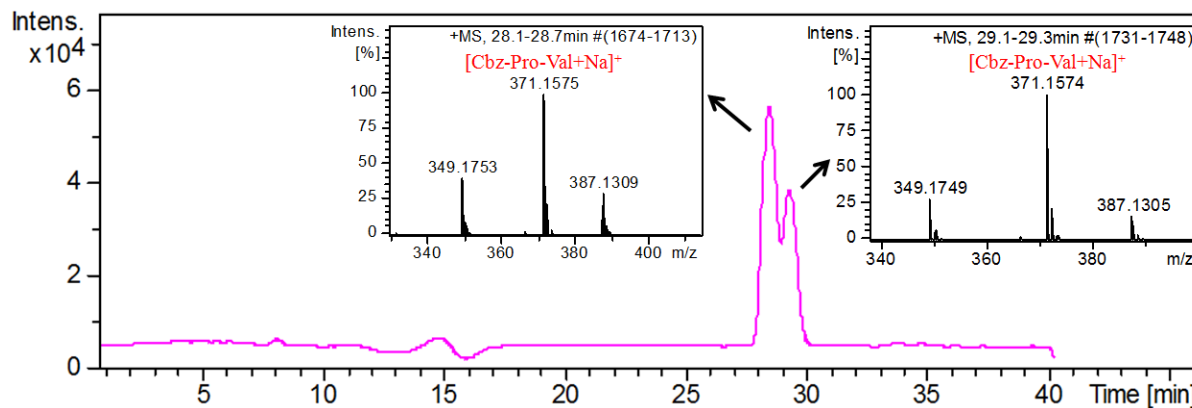


**Figure S19.** LC-MS of Cbz-L-pro-DL-val dipeptide. Both the LC peaks correspond to mass of the dipeptide (calcd  $m/z$  371.1577,  $[M+Na]^+$ ) and seems to be due to Cbz-L-pro-D-val and Cbz-L-pro-L-val.

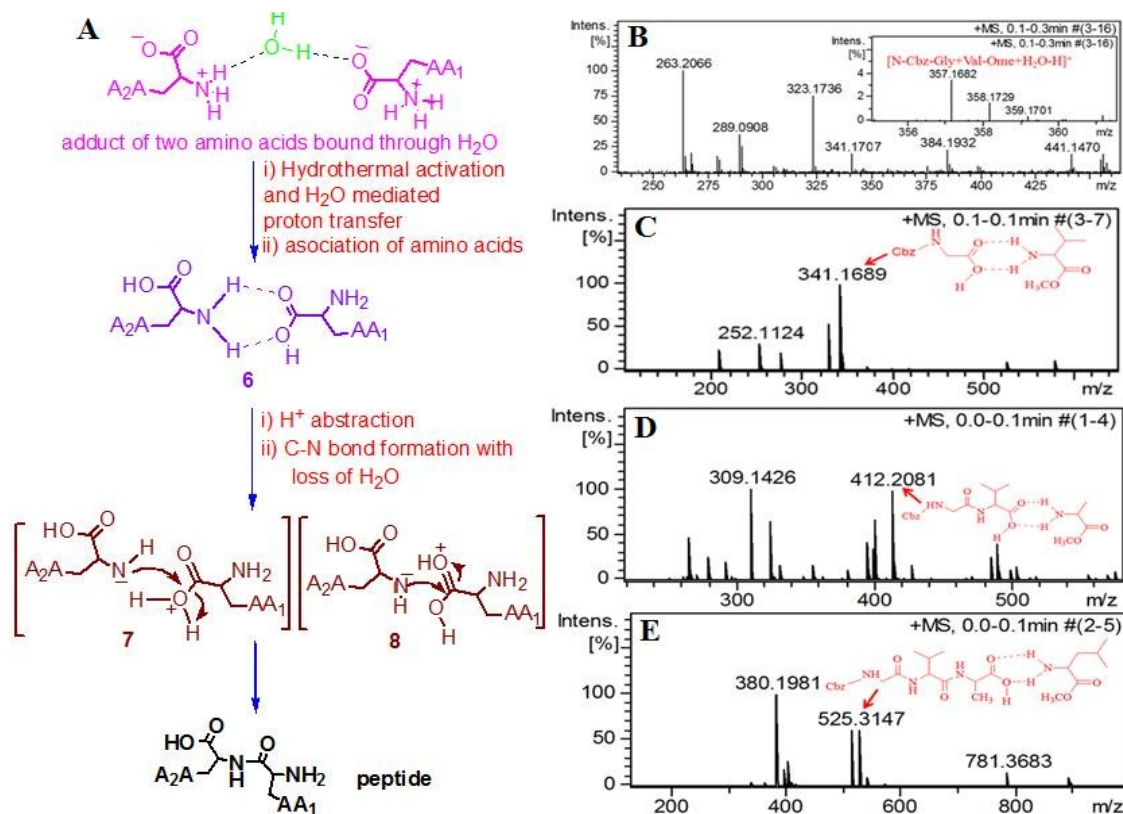


**Figure S20.** (A) Plausible steps for peptide bond formation under un-catalyzed, aqueous phase reaction conditions; (B) HRMS of the reaction mixture of N-Cbz-gly and L-val(OMe).HCl showing association of water molecule with the two reactants,  $m/z$  357.1682 (calcd  $m/z$  357.1656). Peak at  $m/z$  341 and 323 correspond to non-covalent dimer and dipeptide, respectively. HRMS of reaction mixtures showing formation of adduct of: (C) N-Cbz-gly and L-val(OMe) (calcd  $m/z$  341.1707,  $[M+H]^+$ ), (D) N-Cbz-gly-val and L-ala(OMe) (calcd  $m/z$  412.2078,  $[M+H]^+$ ) and (E) N-Cbz-gly-val-ala and L-leu(OMe) (calcd  $m/z$  525.3118,  $[M+H]^+$ ).

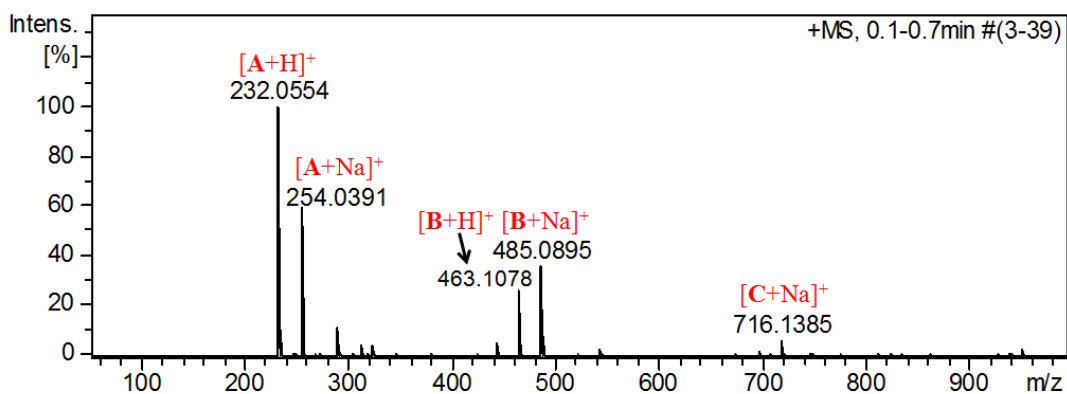


**Figure S21.** Mass spectrum of solution of N-Cbz-gly and ala at pH 8.0-10.0 (refer chart S1 for A-C). There was no mass peak corresponding to the formation of peptide.

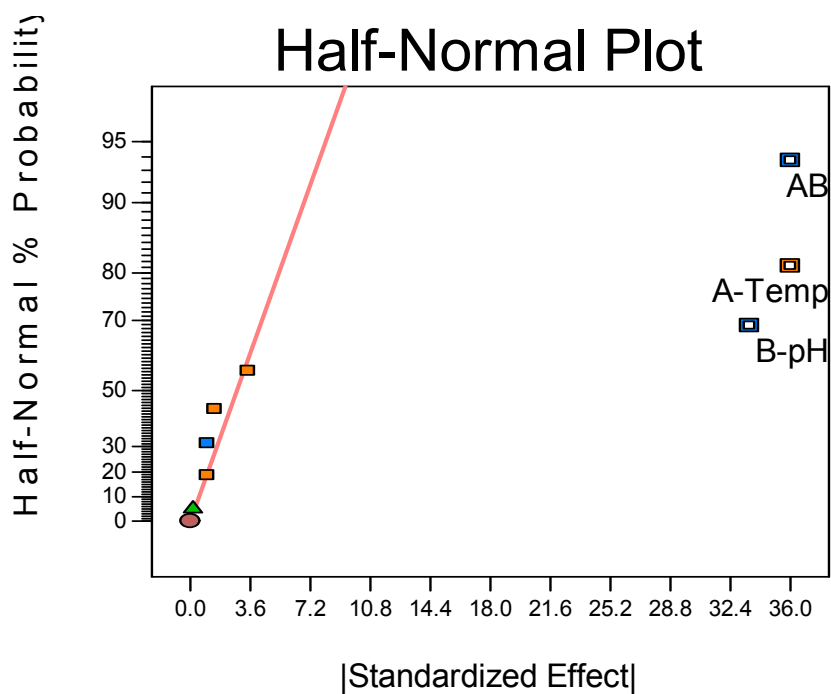


**Figure S22.** Half Normal % Probability graph showing significant process variables.

**Table S1.** Experimental data for reaction temperature, pH, reaction time and reactant concentration for un-catalyzed aqueous phase formation of N-Cbz-val-gly(OMe).

Exp.	Variable 1	Variable 2	Variable 3	Variable 4	Response
No.	Reaction temp (°C)	pH	Reaction time (min)	Concentration (M)	Yield (%)
1	60	3	30	4.7	0
2	70	3	30	4.7	0
3	80	3	30	4.7	0
4	90	3	30	4.7	0
5	100	3	30	4.7	0
6	110	3	30	4.7	0
7	120	3	30	4.7	0
8	100	4	30	4.7	0
9	100	5	30	4.7	0
10	100	6	30	4.7	0
11	100	7	30	4.7	0
12	100	8	30	4.7	0
13	100	9	30	4.7	0
14	100	10	30	4.7	0
15	100	6	60	4.7	0
16	100	6	90	4.7	0
17	100	6	120	4.7	0
18	100	6	150	4.7	0
19	100	6	180	4.7	0
20	100	6	210	4.7	0
21	100	6	240	4.7	3
22	100	6	300	4.7	5
23	110	4	30	4.7	0
24	110	5	30	4.7	0
25	110	6	30	4.7	0
26	110	7	30	4.7	0
27	110	8	30	4.7	0
28	110	9	30	4.7	0
29	110	10	30	4.7	0
30	110	6	60	4.7	0
31	110	6	90	4.7	0
32	110	6	120	4.7	0
33	110	6	150	4.7	0
34	110	6	180	4.7	0
35	110	6	210	4.7	5
36	110	6	240	4.7	10
37	110	6	300	4.7	12
38	120	4	30	4.7	0
39	120	5	30	4.7	0
40	120	6	30	4.7	0

41	120	7	30	4.7	0
42	120	8	30	4.7	0
43	120	9	30	4.7	0
44	120	10	30	4.7	0
45	120	6	60	4.7	0
46	120	6	90	4.7	0
47	120	6	120	4.7	0
48	120	6	150	4.7	0
49	120	6	180	4.7	10
50	120	6	210	4.7	15
51	120	6	240	4.7	20
52	120	6	60	2.38	0
53	120	6	90	2.38	0
54	120	6	120	2.38	0
55	120	6	150	2.38	0
56	120	6	180	2.38	5
57	120	6	210	2.38	10
58	120	6	240	2.38	15
59	120	6	300	2.38	20
60	120	6	60	1.58	0
61	120	6	90	1.58	0
62	120	6	120	1.58	0
63	120	6	150	1.58	0
64	120	6	180	1.58	3
65	120	6	210	1.58	8
66	120	6	240	1.58	11
67	120	6	300	1.58	12
68	120	6	60	0.94	0
69	120	6	90	0.94	0
70	120	6	120	0.94	0
71	120	6	150	0.94	0
72	120	6	180	0.94	0
73	120	6	210	0.94	4
74	120	6	240	0.94	7
75	120	6	300	0.94	10

---

**Table S2.** Fractional factorial design (Resolution-IV) showing four independent variables along with actual and predicted yield

Exp. no.	Point type	Reaction variables (Coded units)				Reaction variables (Actual values)				Response Yield (%)	
		Temp	pH	Time	Conc	Temp (°C)	pH	Time (min)	Conc (M)	Actual	Predicted
1	Factorial	-1	-1	-1	-1	90	5	180	2.5	0	0.1
2	Factorial	1	-1	-1	1	120	5	180	5.0	70	72.0
3	Factorial	-1	1	-1	1	90	7	180	5.0	0	2.5
4	Factorial	1	1	-1	-1	120	7	180	2.5	0	2.5
5	Factorial	-1	-1	1	1	90	5	360	5.0	0	0.1
6	Factorial	1	-1	1	-1	120	5	360	2.5	74	72.0
7	Factorial	-1	1	1	-1	90	7	360	2.5	5	2.5
8	Factorial	1	1	1	1	120	7	360	5.0	5	2.5
9	Center	0	0	0	0	105	6	270	3.75	40	42.0
10	Center	0	0	0	0	105	6	270	3.75	44	42.0

**Table S3.** Comparison of percentage yield and optical rotation of peptides obtained through two different experiments.

Entry	Peptide	Reaction procedure 1 <sup>#</sup>		Reaction procedure 2 <sup>*</sup>	
		% yield	[ $\alpha$ ] <sub>D</sub>	% yield	[ $\alpha$ ] <sub>D</sub>
<b>1</b>	N-Cbz-gly-ala(OMe)	75	-10°	62	-12°
<b>2</b>	N-Cbz-val-gly(OMe)	74	-20°	60	-21°
<b>3</b>	N-Cbz-gly-val(OMe)	75	-20°	64	-19°
<b>4</b>	N-Cbz-pro-leu(OMe)	70	-40°	62	-38°
<b>5</b>	N-Cbz-pro-ala(OMe)	68	-30°	58	-30°
<b>6</b>	N-Cbz-val-gly-leu(OMe)	70	-34°	52	-33°
<b>7</b>	N-Cbz-gly-val-ala	60	-40°	50	-42°
<b>8</b>	N-Cbz-gly-val-ala(OMe)	65	-40°	54	-40°
<b>9</b>	N-Cbz-gly-ala-pro	68	-30°	55	-25°
<b>10</b>	N-Cbz-val-gly-leu-ala(OMe)	67	-40°	48	-42°

<sup>#</sup>heating aqueous mixture of N-Cbz-amino acid/peptide with amino acid at 110-120 °C, pH 5.0; <sup>\*</sup>reaction in CHCl<sub>3</sub> in presence of ethyl chloroformate, triethyl amine

**Table S4.** ANOVA table and model statistics for yield

Source	Sum of Squares	df	Mean Square	F-Value	p-value Prob. > F
Model	7414.1	3	2471.3	17.1	0.0024*
A-Temp	2584.8	1	2584.8	17.9	0.0055*
B-pH	2244.5	1	2244.5	15.5	0.0076*
A x B	2584.8	1	2584.8	17.9	0.0055*
<i>Lack of Fit</i>	856.4	5	171.2	21.4	0.1626#
<b><u>Model diagnostic</u></b>					
	Std. Dev.	12.00		R <sup>2</sup>	0.895
	Mean	23.84		Adj. R <sup>2</sup>	0.843
	C.V. %	50.35		Pred R <sup>2</sup>	0.814

\* significant at p<0.05

# not- significant at p<0.05

### **General experimental procedure for reactions performed under hydrothermal conditions**

Solution of two amino acids in ultrapure water (Sigma-Aldrich) was taken in a round bottom flask. Starting from 50 °C, the reaction temperature was increased in steps of 10 °C and at each temperature, it was heated for 5h. Concentration and pH were the other two variables which were taken into consideration. The progress of the reaction was monitored by taking out a small part of the reaction mixture after every 20 min and recording the high resolution mass spectra. The reaction mentioned below correspond to aqueous phase reaction performed under optimized reaction conditions.

**N-Cbz-Val-Gly-Leu-Ala-OMe.** Mixture of N-Cbz-valine (500 mg) and glycine methyl ester hydrochloride (251 mg) in 1 ml H<sub>2</sub>O was heated at 120 °C for 6 h. Formation of N-Cbz-gly-pro methyl ester dipeptide was confirmed from HRMS. 5% Na<sub>2</sub>CO<sub>3</sub> solution was added to the reaction mixture and extracted with ethyl acetate. The organic layer was dried over anhydrous Na<sub>2</sub>SO<sub>4</sub> and evaporated under vacuum to get thick liquid which was purified over

flash chromatography (ethyl acetate-hexane) to get pure N-Cbz-val-gly methyl ester. Hydrolysis of N-Cbz-gly-pro methyl ester with 1N NaOH in acetone-water provided N-Cbz-gly-pro dipeptide (485 mg, 74%). Further, mixture of N-Cbz-val-gly dipeptide (485 mg) and L-leucine methyl ester (190 mg) in 1 ml H<sub>2</sub>O was heated at 120 °C for 6 h. After usual work up and followed by hydrolysis of N-Cbz-val-gly-leu-OMe (70%) with 1N NaOH in acetone-water provided N-Cbz-val-gly-leu tripeptide (310 mg, 45%). Next, aqueous solution of N-Cbz-val-gly-leu tripeptide (310 mg) and L-alanine methyl ester (253 mg) was heated at 120 °C for 6 h and N-Cbz-val-gly-leu-ala methyl ester was obtained. 5% Na<sub>2</sub>CO<sub>3</sub> solution was added to the reaction mixture and extracted with ethyl acetate. The organic layer was dried over anhydrous Na<sub>2</sub>SO<sub>4</sub> and evaporated under vacuum to get thick liquid which was purified over flash chromatography (ethyl acetate-methanol) to get pure N-Cbz-val-gly-leu-ala methyl ester (67%). HRMS (*m/z*): [M+H]<sup>+</sup> calcd for C<sub>25</sub>H<sub>38</sub>N<sub>4</sub>O<sub>7</sub>, 507.2815, found 507.2844. The purity / chiral purity of the tetrapeptide was ascertained with the help of LC-MS and it was characterized with NMR spectral data. During all these reactions, the pH was maintained at 5.0.

**gly-pro-val-ala-ile.** Mixture of N-Cbz-glycine (500 mg) and L-proline methyl ester hydrochloride (309 mg) in 1 ml H<sub>2</sub>O was heated at 120 °C for 6 h. Formation of N-Cbz-gly-pro methyl ester dipeptide was confirmed from HRMS. 5% Na<sub>2</sub>CO<sub>3</sub> solution was added to the reaction mixture and extracted with ethyl acetate. The organic layer was dried over anhydrous Na<sub>2</sub>SO<sub>4</sub> and evaporated under vacuum to get thick liquid which was purified over flash chromatography (ethyl acetate-hexane) to get pure N-Cbz-gly-pro methyl ester. Hydrolysis of N-Cbz-gly-pro methyl ester with 1N NaOH in acetone-water provided N-Cbz-gly-pro dipeptide (620 mg, 80%). Further, mixture of N-Cbz-gly-pro dipeptide (620 mg) and L-valine methyl ester (264 mg) in 1 ml H<sub>2</sub>O was heated at 120 °C for 6 h. After usual work up and followed by hydrolysis of N-Cbz-gly-pro-val-OMe with 1N NaOH in acetone-water provided N-Cbz-gly-pro-val tripeptide (370 mg, 45%). Next, aqueous solution of N-Cbz-gly-pro-val tripeptide (370 mg) and L-alanine methyl ester (253 mg) was heated at 120 °C for 6 h. Again after usual work up and hydrolysis of N-Cbz-gly-pro-val-ala-OMe with 1N NaOH in acetone-water, N-Cbz-gly-pro-val-ala tetrapeptide (170 mg, 35%) was procured. Finally, mixture of N-Cbz-gly-pro-val-ala tetrapeptide (170 mg) and L-isoleucine methyl ester (48 mg) was heated at 120 °C for 5 h. Formation of N-Cbz-gly-pro-val-ala-ile methyl ester pentapeptide was confirmed from HRMS. 5% Na<sub>2</sub>CO<sub>3</sub> solution was added to the reaction mixture and extracted with ethyl acetate. The organic layer was dried over anhydrous Na<sub>2</sub>SO<sub>4</sub> and evaporated under vacuum to get thick liquid which was purified over flash



chromatography (ethyl acetate-methanol) to get pure N-Cbz-gly-pro-val-ile methyl ester. Hydrolysis of N-Cbz-gly-pro-val-ala-ile methyl ester with 1N NaOH in acetone-water provided N-Cbz-gly-pro-val-ala-ile pentapeptide (60 mg, 55%,  $[\alpha]_D = -55^\circ$  (1, MeOH)). To the solution of N-Cbz-gly-pro-val-ala-ile pentapeptide (40 mg) in 0.5 ml methanol added 0.2 ml glacial acetic acid, 8 mg Pd/C and passed H<sub>2</sub> gas for 3h. The reaction mass was filtered and concentrated to obtain gly-pro-val-ala-ile pentapeptide (35 mg, 92%). HRMS ( $m/z$ ):  $[M+H]^+$  calcd for C<sub>21</sub>H<sub>37</sub>N<sub>5</sub>O<sub>6</sub>, 456.2816, found 456.2809. The purity / chiral purity of the pentapeptide was ascertained with the help of LC-MS and it was characterized with NMR spectral data. pH was maintained at 5.0 during all the steps.

**his, pro, arg, lys tetrapeptide.** Solution of L-his.HCl (500 mg) and L-pro (302 mg) in distilled water (0.5 ml) (pH 5.5) was heated at 120 °C for 5h. Formation of pro-his/his-pro dipeptide was confirmed from HRMS of the reaction mixture. Further, l-arg.HCL (542 mg) was added to the above solution and continue heating for another 5h at 120 °C maintaining pH 5.0. The formation of tripeptide of pro, his and arg was confirmed from HRMS of the reaction mixture. To the solution of pro, his, arg tripeptide in 0.5 ml distilled water, L-lys.HCl (356 mg) was added. pH of the solution was adjusted at 5.0. The reaction mixture was heated at 120 °C for 5h. Formation of tetrapeptide was detected from HRMS of the reaction mixture (Scheme S1). HRMS ( $m/z$ ):  $[M+H]^+$  calcd for C<sub>23</sub>H<sub>40</sub>N<sub>10</sub>O<sub>5</sub>, 537.3155, found 537.3161. The percentage formation of the di-, tri- and tetra- peptides was calculated by dividing the peak intensity of the peptide with sum of intensities of all the peaks in the mass spectrum.

**Peptide synthesis under conventional conditions.** 500 mg of N-Cbz-val was dissolved in 5 ml dry chloroform containing 0.33 ml dried triethylamine. Reaction mixture was cooled in ice and 0.30 ml ethylchloroformate was added followed by the addition of 285 mg L-gly methyl ester hydrochloride in 5 ml chloroform containing a further 0.5 ml triethylamine. Stirred the reaction mixture at room temperature for 4h. Chloroform was evaporated and the reaction mass was washed with 10% HCl solution and 10% NaHCO<sub>3</sub> solution and extracted with ethyl acetate. The crude product obtained after removal of ethyl acetate was purified by column chromatography using ethyl acetate-hexane (2:8) as eluent to procure pure N-Cbz-val-gly methyl ester (650 mg) ( $[\alpha]_D = -21^\circ$  (1, CHCl<sub>3</sub>)). N-Cbz-val-gly methyl ester was dissolved in 5 ml acetone-H<sub>2</sub>O (2:1) and added 1.5 ml 1N NaOH and stirred for 1h at room temperature to obtain N-Cbz-val-gly dipeptide. Using the same experimental protocol, N-Cbz-val-gly-leu-val(OMe) ( $[\alpha]_D = -42^\circ$  (1, CHCl<sub>3</sub>)) tetrapeptide was obtained.

## Experimental design and model development

Fractional factorial design ( $2^{4-1}$ ) was used to screen four independent process variables viz. (i) reaction temperature (90 °C – 120 °C), (ii) pH (5 – 7), (iii) reaction time (180 min – 360 min) and concentration of reactants (2.5 M – 5.0 M) as per Resolution-IV design. This is the minimum experimental run design to allow all main effects to be estimated and along with two factor interactions (2FI). Although, 2FI is aliased with each other. Experimental design consisting of 8 factorial points and 2 center runs is given in table S2. The experimental runs were conducted in a randomized manner to guard against systematic bias. Each process variable is coded +1 for maximum process range and -1 as minimum process range. Maximum yield (74%) was obtained at 120 °C, pH of 5, 360 min and 2.5 M reactant concentration. Half normal plot was used for selecting significant process variables (Figure S22). After selection of important variables based on t-values and Bonferroni limits, the analysis of variance (ANOVA) model was generated along with its significance level. The ANOVA model was significant at p-value=0.0024 (F-value= 17.1, degree of freedom=3) with non-significant lack of fit (p=0.1626) (Table S4). Model *Goodness of fit* was checked through Normal plot of residuals, coefficient of determination ( $R^2= 0.895$ ) and strong signal to noise (S/N) ratio as given by Adequate Precision of 9.47 (>4 is considered satisfactory). Although, coefficient of variation (CV) is on higher side (50.35%) due to very high ratio of maximum to minimum response (740), which otherwise indicated of response transformation. Although, square root transformation improves the CV but deteriorate the Normal probability plot for the yield. Thus, model was generated without transformation.

Model fitting and graphical analyses were carried out using the Design-Expert software v9.0 (Stat-Ease Inc., Minneapolis, USA). The selected models were generated both in terms of coded factors (standardized equations) and actual factors (unstandardized equations) as given in Eq.(1) and Eq.(2) respectively. The regression constants in the coded equation are unitless coefficients and are used for process understanding.

$$\text{Yield (\%)} = + 23.84 + 17.98 A - 16.75 B - 17.98 A \times B \quad (1)$$

where A: Reaction temperature and B: pH are in coded units.

$$\text{Yield (\%)} = - 756.435 + 8.388 A + 109.075 B - 1.198 A \times B \quad (2)$$

where A: Reaction temperature (°C) and B: pH are in actual units.

There is strong two factor interaction (2FI) between reaction temperature and pH, this antagonist interaction is more significant as temperature increases from 90°C to 120 °C. The model developed was subjected to yield maximization and predicted 76.5% yield. A validation experiment was performed at 120 °C, pH=5, 270 min reaction time and 3.75 M reactant concentration gave a yield of 76% to validate the model significance and for confirmation of the model.